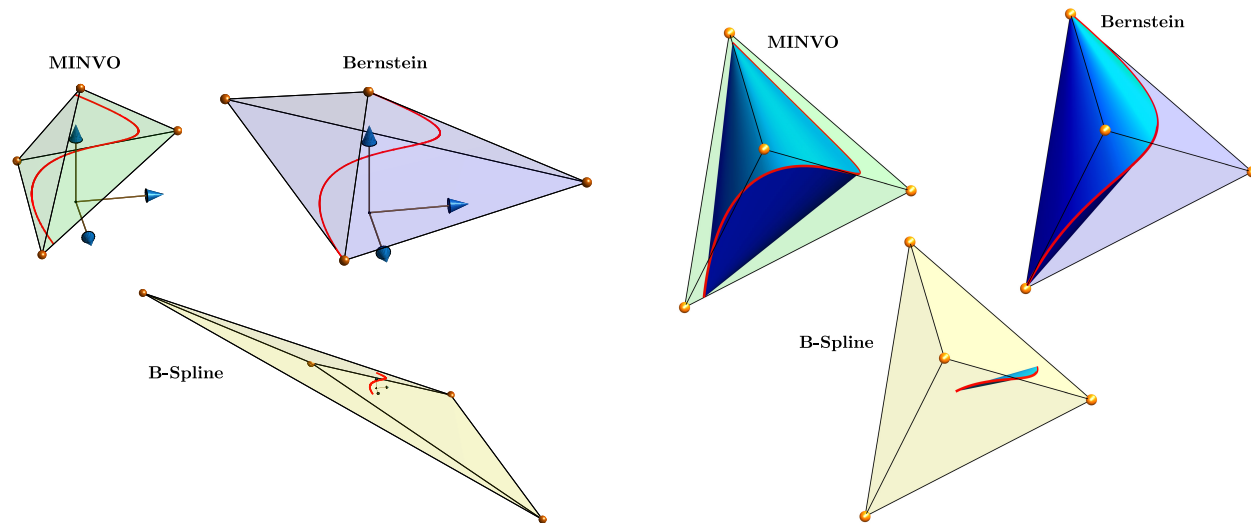


MINVO Basis: Finding Simplexes with Minimum Volume Enclosing Polynomial Curves

JESUS TORDESILLAS, Massachusetts Institute of Technology
JONATHAN P. HOW, Massachusetts Institute of Technology



(a) For **any** given 3rd-order polynomial curve, the MINVO basis finds an enclosing 3-simplex that is 2.36 and 254.9 times smaller than the one found by the Bernstein and B-Spline bases respectively.

(b) For **any** given 3-simplex, the MINVO basis finds a 3rd-order polynomial curve inscribed in the simplex, and whose convex hull is 2.36 and 254.9 times larger than the one found by the Bernstein and B-Spline bases respectively.

Fig. 1. Comparison between the MINVO, Bernstein and B-Spline bases for $n = 3$. The MINVO basis obtains globally optimal results for $n = 1, 2, 3$.

Outer polyhedral representations of a given polynomial curve are extensively exploited in computer graphics rendering, computer gaming, path planning for robots, and finite element simulations. Bézier curves (which use the Bernstein basis) or B-Splines are a very common choice for these polyhedral representations because their non-negativity and partition-of-unity properties guarantee that each interval of the curve is contained inside the convex hull of its control points. However, the convex hull provided by these bases is not the one with smallest volume, producing therefore undesirable levels of conservatism in all of the applications mentioned above. This paper presents the MINVO basis, a polynomial basis that generates the smallest n -simplex that encloses *any* given n^{th} -order polynomial curve. The results

obtained for $n = 3$ show that, for *any* given 3rd-order polynomial curve, the MINVO basis is able to obtain an enclosing simplex whose volume is 2.36 and 254.9 times smaller than the ones obtained by the Bernstein and B-Spline bases, respectively. When $n = 7$, these ratios increase to 902.7 and $2.997 \cdot 10^{21}$, respectively. Moreover, we show that the MINVO basis also solves for the n^{th} -order polynomial curve with the largest convex hull enclosed in *any* given n -simplex. Global optimality is discussed and proven for $n = 1, 2, 3$ using Sum-Of-Squares (SOS) Programming, branch and bound, and moment relaxations.

CCS Concepts: • **Computing methodologies** → **Computer graphics**; • **Mathematics of computing** → **Nonconvex optimization**.

Additional Key Words and Phrases: Polynomial basis, Minimum inscribing simplex, Largest convex hull, Polynomial curves, Bernstein, B-Splines

ACM Reference Format:

Jesus Tordesillas and Jonathan P. How. 2020. MINVO Basis: Finding Simplexes with Minimum Volume Enclosing Polynomial Curves. 1, 1 (December 2020), 17 pages. <https://doi.org/00.0000/0000000.0000000>

Supplementary material:

- **Code:** <https://github.com/mit-acl/minvo> (to appear soon)
- **Video:** https://www.youtube.com/watch?v=f_JOYud9LUU

Authors' addresses: Jesus Tordesillas, jtorde@mit.edu, Massachusetts Institute of Technology, 77 Massachusetts Ave., Cambridge, Massachusetts, 02139; Jonathan P. How, jhow@mit.edu, Massachusetts Institute of Technology, 77 Massachusetts Ave., Cambridge, Massachusetts, 02139.

Permission to make digital or hard copies of all or part of this work for personal or classroom use is granted without fee provided that copies are not made or distributed for profit or commercial advantage and that copies bear this notice and the full citation on the first page. Copyrights for components of this work owned by others than ACM must be honored. Abstracting with credit is permitted. To copy otherwise, or republish, to post on servers or to redistribute to lists, requires prior specific permission and/or a fee. Request permissions from permissions@acm.org.

© 2020 Association for Computing Machinery.

XXXX-XXXX/2020/12-ART \$15.00

<https://doi.org/00.0000/0000000.0000000>

1 INTRODUCTION

Bézier and B-Spline curves are extensively used in many different applications, including computer aided design [Autocad® 2020; De Kemp 1999; Dimas and Briassoulis 1999; Inventor® 2020; Maya® 2020], simulations and animations [Bargteil and Cohen 2014; Roth et al. 1998], and robotics [Faraway et al. 2007; Jolly et al. 2009; Park and Ravani 1995; Preiss et al. 2017; Sahingoz 2014; Škrjanc and Klančar 2010; Tordesillas et al. 2019]. The ability to approximate the space occupied by a given polynomial curve with a polyhedron is crucial for many of these applications, especially those that need to check the intersection between two objects in real time. For instance, many path planning algorithms that use Bézier curves can easily guarantee safety by ensuring that the control points of each interval of the trajectory are inside the polyhedra that define the free space [Preiss et al. 2017; Sahingoz 2014; Tordesillas et al. 2019]. This allows the imposition of a finite number of constraints only on the vertexes of this outer polyhedral representation of the interval, instead of an infinite number of constraints at all of the points in each interval. Moreover, the convex hull property of Bézier curves can also be exploited to compute curve intersections, perform ray tracing or to compute minimum distances between convex shapes [Cichella et al. 2017; Efremov et al. 2005; Gilbert et al. 1988; Schulz 2009; Sederberg and Nishita 1990]. Other applications that benefit from having a polyhedral outer approximation of a curve are envelope approximations in optimization [Dang and Testylier 2012; Garloff and Smith 2003; Löfberg 2020], control and safety for dynamical systems [Kuti et al. 2014], and certified robustness in neural networks that use polynomials as the input [Everett et al. 2020; Wong and Kolter 2018].

While having other useful properties, neither the Bernstein basis (polynomial basis used by Bézier curves) nor the B-Spline basis generate the smallest simplex that encloses a given interval of the curve. This directly translates into an unnecessary conservatism in many of the aforementioned applications. The goal of this paper is to obtain the polynomial basis that generates the simplex with minimum volume that encloses a given polynomial curve. Moreover, we show that this polynomial basis can also be used to obtain the polynomial curve with largest convex hull enclosed in a given simplex.

The contributions of this paper are summarized as follows:

- Formulation of the general optimization problem that solves for the smallest n -simplex that encloses **any** given n^{th} -order polynomial curve. We show that this formulation also solves for the n^{th} -order polynomial curve with largest convex hull enclosed in **any** given n -simplex. A more tractable formulation by imposing a specific structure in the polynomials of the basis is also presented.
- We derive the results for $n = 1, 2, \dots, 7$, obtaining simplexes that, for $n = 3$, are always 2.36 and 254.9 times smaller than the ones obtained using the Bernstein and B-Spline bases respectively. For $n = 7$, these values increase to 902.7 and $2.997 \cdot 10^{21}$ respectively.
- Global optimality is proven for $n = 1, 2, 3$ using SOS, branch and bound, and moment relaxations.
- Extension of the MINVO basis to general polynomial curves and surfaces, and to some rational curves.

2 RELATED WORK

The work by Herron [Herron 1989] attempted to find for $n = 2$ and $n = 3$ the smallest n -simplex enclosing an n^{th} order polynomial curve. The approach of this work was to impose a specific structure on the polynomials of the basis, and then solve the associated non-convex optimization problem over the roots of those polynomials. For this specific structure of the polynomials, a global minimizer was found for $n = 2$, and a local minimizer was found for $n = 3$. However, global optimality over all possible polynomials was not proven, and only the cases $n = 2$ and $n = 3$ were studied. Similarly, in the results of [Kuti et al. 2014], Kuti et al. use the algorithm proposed in [Li and Bioucas-Dias 2008] to obtain a minimal 2-simplex that encloses a specific 2nd-order polynomial curve. However, this approach requires running the algorithm for *each* different curve, no global optimality is shown, and only one case with $n = 2$ was analyzed. In contrast to these works, our paper presents the most general formulation that scales to any n and does not lose generality by imposing an ad-hoc structure on the polynomials of the basis. For this general case, we get globally optimal results for $n = 1, 2, 3$, locally optimal results for $n = 4$ and feasible solutions for $n = 5, 6, 7$. Then, by imposing a specific structure on the basis functions, we obtain globally optimal solutions for $n = 1, 2, 3$ and locally optimal solutions for $n = 4, 5, 6, 7$.

Some works have focused on the properties of the smallest n -simplex that encloses a given generic convex body. [Gálcer et al. 2019; Kanazawa 2014] derived some bounds for the volume of this simplex, while Klee showed in [Klee 1986] that any locally optimal simplex (with respect to its volume) that encloses a convex body must be a centroidal simplex. In other words, the centroid of its facets must belong to the convex body. Applied to a curve P , this would mean that the centroid of its facets must belong to $\text{conv}(P)$. Although this is a necessary condition, it is *not* sufficient for local optimality.

When the convex body is a polyhedron (or equivalently the convex hull of a finite set of points), [Vegter and Yapy 1993] classifies the possible minimal circumscribing simplexes, and this classification is later used by [Zhou and Suri 2002] to derive a $O(k^4)$ algorithm that computes the smallest simplex enclosing a finite set of k points. This problem is also crucial for the hyperspectral unmixing in remote sensing, to be able to find the proportions (or abundances) of each macroscopic materials (endmembers) contained in a given image pixel [Hendrix et al. 2013; Uezato et al. 2019], and many different iterative algorithms have been proposed towards this end [Iordache et al. 2009; Rogge et al. 2006; Velez-Reyes et al. 2003]. All these works focus on generic set of points that are not necessarily sampled from a polynomial curve, and that is what leads to the need of iterative algorithms. Our work focuses instead on polynomial curves, and solves the problem without any discretization of points along the curve.

The convex hull of curves has also been studied in the literature. [Derry 1956; Ranestad and Sturmfels 2009; Sedykh 1986] studied the boundaries of these convex hulls, while [Ciripoi et al. 2018] focused on the patches of the convex hull of trajectories of polynomial dynamical systems. For a moment curve $[t \ t^2 \ \dots \ t^n]^T$ (where t is in some closed interval), [Mazur 2017] found that the number of

points needed to represent every point in the convex hull of this curve is $\frac{n+1}{2}$, giving therefore a tighter bound than the $(n+1)$ points found using by the Carathéodory's Theorem [Carathéodory 1907; Steinitz 1913]. This particular curve, and the volume of its convex hull, were also analyzed by [Karlin and Shapley 1953] in the context of moment spaces and orthogonal polynomials. Although many useful properties of the convex hull of a curve are shown in all these previous works, none of them addresses the problem of finding the polynomial curve with largest convex hull enclosed in a given simplex.

3 PRELIMINARIES

3.1 Notation and Definitions

The notation used throughout the paper is summarized in Table 1. Unless otherwise noted, all the indexes in this paper will start at 0. For instance, $M_{0,3}$ is the fourth element of the first row of the matrix M . Let us also introduce the two following common definitions and their respective notations.

n -simplex: Convex hull of $n+1$ points $v_0, \dots, v_n \in \mathbb{R}^n$. These points are **vertexes** of the simplex, and will be stacked in the **matrix of vertexes** $V := [v_0 \dots v_n]$. The letter S will denote a particular simplex, while S^n will denote the set of all possible n -simplexes. A simplex with $V = [0 \ I_n]$ will be called the **standard n -simplex**.

Polynomial curve P of degree n and dimension k :

$$P := \{p(t) \mid t \in [a, b], a \in \mathbb{R}, b \in \mathbb{R}, b > a\}$$

where $p(t) := \begin{bmatrix} p_0(t) \\ \vdots \\ p_{k-1}(t) \end{bmatrix} := Pt \in \mathbb{R}^k$, with $p_i(t)$ a polynomial



of degree n . The matrix P is the coefficient matrix, and will be denoted as $P_{k \times (n+1)} := [p_n \dots p_0]$. As in this paper we use the spatial curve, and not the specific parametrization of the curve, without loss of generality we will use the interval $t \in [-1, 1]$ (i.e., $a = -1$ and $b = 1$), and assume that the parametrization of $p(t)$ has minimal degree (i.e. no other polynomial parametrization with lower degree produces the same spatial curve P). The subspace containing P and that has the smallest dimension will be denoted as $M \subseteq \mathbb{R}^k$, and its dimension will be m . We will work with the case $n = m = k$ (and refer to such curves simply as **n^{th} -order polynomial curves**). The set of all possible n^{th} -order polynomial curves will be denoted as \mathcal{P}^n . Section 7 will then extend the results to curves with arbitrary n , m and k .

We will use the basis matrix of a segment of a non-clamped uniform B-Spline for comparison [Qin 2000, Section 4.1], and refer to this basis simply as the **B-Spline basis**.

3.2 Volume of the Convex Hull of a Polynomial Curve

At several points throughout the paper, we will make use of the following theorem, that we prove in the Appendix (Section A):

Table 1. Notation used in this paper.

Symbol	Meaning
$a, \mathbf{a}, \mathbf{A}$	Scalar, column vector, matrix
$ A , \text{tr}(\mathbf{A})$	Determinant of \mathbf{A} , trace of \mathbf{A}
$\text{abs}(a)$	Absolute value of a
\mathbf{t}	$[t^r \ t^{r-1} \dots \ 1]^T$ (r given by the context)
$\hat{\mathbf{t}}$	$[1 \dots t^{r-1} \ t^r]^T$ (r given by the context)
$\mathbf{p}(t)$	Column vector whose entries are polynomials in t
P	Polynomial curve $P := \{p(t) \mid t \in [-1, 1]\}$
\mathbf{P}	Coefficient matrix of P . $p(t) = Pt$
\mathcal{P}^n	Set of all possible n -th order polynomial curves
$\text{conv}(P)$	Convex hull of P
n	Maximum degree of the entries of $\mathbf{p}(t)$
k	Number of rows of $\mathbf{p}(t)$
\mathcal{M}	Subspace with the smallest dimension that contains P . $\mathcal{M} \subseteq \mathbb{R}^k$
m	Dimension of \mathcal{M}
S	Simplex
S^n	Set of all possible n -simplexes
V	Matrix whose columns are the vertexes of a simplex
$\partial \cdot$	Frontier of a set
$\propto, \mathbf{1}, \mathbf{0}, \mathbf{a} \geq \mathbf{b}$	Proportional to, column vector of ones, column vector of zeros, element-wise inequality
$\cdot_{a \times b}$	Size of a matrix (a rows \times b columns)
\mathbf{e}	$[0 \ 0 \dots \ 0 \ 1]^T$ (size given by the context)
\mathbf{I}_n	Identity matrix of size $n \times n$
$M_{:,c:d}$	Matrix formed by columns $c, c+1, \dots, d$ of M
\mathbb{S}_+^a	Positive semidefinite cone (set of all symmetric positive semidefinite $a \times a$ matrices)
$\text{vol}(\cdot)$	Volume (Lebesgue measure)
π	Hyperplane
$\text{dist}(\mathbf{a}, \pi)$	Distance between the point \mathbf{a} and the hyperplane π
MV, Be, BS	MINVO, Bernstein and B-Spline respectively
	Color notation for the MINVO, Bernstein and B-Spline bases respectively
	Color notation for Problem 1, 2, 3 and 4 respectively

Theorem 1: The volume of the convex hull of $P \in \mathcal{P}^n$ ($t \in [-1, 1]$), is given by:

$$\text{vol}(\text{conv}(P)) = \frac{\text{abs}(|P_{:,0:n-1}|)}{n!} 2^{\frac{n(n+1)}{2}} \prod_{0 \leq i < j \leq n} \left(\frac{j-i}{j+i} \right)$$

Proof: See Appendix (Section A). \square

Note that, as the curve P satisfies $n = m = k$ (see Section 3.1), the volume of its convex hull is nonzero and therefore $|P_{:,0:n-1}| \neq 0$.

4 PROBLEMS DEFINITION

As explained in Section 1, the goal of this paper is to find the smallest simplex $S \in \mathcal{S}^n$ enclosing a given polynomial curve $P \in \mathcal{P}^n$, and to find the polynomial curve $P \in \mathcal{P}^n$ with largest convex hull enclosed in a given simplex $S \in \mathcal{S}^n$.

4.1 Given $P \in \mathcal{P}^n$, find $S \in \mathcal{S}^n$

Problem 1: Given the polynomial curve $P \in \mathcal{P}^n$, find the simplex $S \in \mathcal{S}^n$ with minimum volume that contains P . In other words:

$$\begin{aligned} \min_{S \in \mathcal{S}^n} \quad f_1 &:= \text{vol}(S) \propto \text{abs} \left(\begin{bmatrix} V^T & 1 \end{bmatrix} \right) \\ \text{s.t.} \quad & P \subset S \end{aligned}$$

For $n = 2$, Problem 1 tries to find the triangle with the smallest area that contains the curve

$$\left\{ \begin{bmatrix} x(t) & y(t) \end{bmatrix}^T \mid t \in [-1, 1] \right\}$$

where $x(t)$ and $y(t)$ are 2nd-degree polynomials in t . For $n = 3$, it tries to find the tetrahedron with the smallest volume that contains the curve

$$\left\{ \begin{bmatrix} x(t) & y(t) & z(t) \end{bmatrix}^T \mid t \in [-1, 1] \right\}$$

where $x(t)$, $y(t)$ and $z(t)$ are 3rd-degree polynomials in t . Similar geometric interpretations apply for higher n .

Note that, as the volume of the convex hull of P is nonzero (see Section 3.2) the volume of the enclosing simplex is also nonzero, and therefore $\left\| \begin{bmatrix} V^T & 1 \end{bmatrix} \right\| \neq 0$.

4.2 Given $S \in \mathcal{S}^n$, find $P \in \mathcal{P}^n$

Problem 2: Given a simplex $S \in \mathcal{S}^n$, find the polynomial curve $P \in \mathcal{P}^n$ contained in S , whose convex hull has maximum volume:

$$\begin{aligned} \min_{P \in \mathcal{P}^n} \quad f_2 &:= -\text{vol}(\text{conv}(P)) \propto -\text{abs} \left(\begin{bmatrix} P_{:,0:n-1} \end{bmatrix} \right) \\ \text{s.t.} \quad & P \subset S \end{aligned}$$

Another geometric interpretation of Problem 2 is that we are trying to find the polynomial curve $P \in \mathcal{P}^n$ contained in a given simplex $S \in \mathcal{S}^n$, whose coefficients vectors $\mathbf{p}_n, \dots, \mathbf{p}_1$ span a parallelogram with largest volume.

We will assume that the matrix of vertexes of the simplex S given satisfies $\left\| \begin{bmatrix} V^T & 1 \end{bmatrix} \right\| \neq 0$. In other words, the simplex S given is not contained in a subspace \mathbb{R}^m , with $m < n$. Now note that the optimal solution for this problem is guaranteed to satisfy $\left| P_{:,0:n-1} \right| \neq 0$, which can be easily proven by noting that we are maximizing the absolute value of $\left| P_{:,0:n-1} \right|$, and that there exists at least one feasible solution (for example the Bézier curve whose control points are the vertexes of S) with $\left| P_{:,0:n-1} \right| \neq 0$.

5 EQUIVALENT FORMULATION

Let us now study the constraints and the objective functions of Problems 1 and 2.

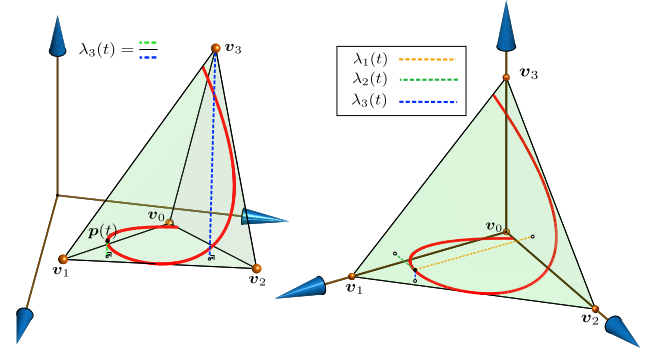


Fig. 2. Geometric interpretation of $\lambda_i(t)$. Each $\lambda_i(t)$ represents the distance from the curve $\mathbf{p}(t)$ and the hyperplane formed by the vertexes $\{v_0, v_1, \dots, v_n\} \setminus v_i$, divided by the distance from the vertex v_i to that hyperplane (left). For the standard 3-simplex in 3D (i.e., $V = \begin{bmatrix} 0 & I_3 \end{bmatrix}$), the curve in red has $\mathbf{p}(t) = [\lambda_1(t) \ \lambda_2(t) \ \lambda_3(t)]^T$ (right).

5.1 Constraints of Problem 1 and 2

Both problems share the same constraint $P \subset S$ (i.e., $\mathbf{p}(t) \in S \ \forall t \in [-1, 1]$), which is equivalent to $\mathbf{p}(t)$ being a convex combination of the vertexes v_i of the simplex for $t \in [-1, 1]$:

$$P \subset S \equiv \left\{ \begin{array}{l} \mathbf{p}(t) = \sum_{i=0}^n \lambda_i(t) \mathbf{v}_i \\ \sum_{i=0}^n \lambda_i(t) = 1 \quad \forall t \\ \lambda_i(t) \geq 0 \quad \forall i = 0, \dots, n \quad \forall t \in [-1, 1] \end{array} \right\} \quad (1)$$

The variables $\lambda_i(t)$ are usually called barycentric coordinates [Ericson 2004], and their geometric interpretation is as follows. Let us first define π_i as the hyperplane that passes through the points $\{v_0, v_1, \dots, v_n\} \setminus v_i$, and \mathbf{n}_i as its normal vector that satisfies the condition $\mathbf{n}_i^T \mathbf{p}(t) > 0$ (i.e., pointing towards the interior of the simplex). Choosing now $q \in \{0, \dots, n\} \setminus i$, and using the fact that $\sum_{j=0}^n \lambda_j(t) = 1$, we have that:

$$\mathbf{p}(t) = \sum_{j=0}^n \lambda_j(t) \mathbf{v}_j = \mathbf{v}_q + \sum_{j=0}^n \lambda_j(t) (\mathbf{v}_j - \mathbf{v}_q)$$

Therefore:

$$\begin{aligned} \text{dist}(\mathbf{p}(t), \pi_i) &:= (\mathbf{p}(t) - \mathbf{v}_q)^T \mathbf{n}_i = \sum_{j=0}^n \lambda_j(t) (\mathbf{v}_j - \mathbf{v}_q)^T \mathbf{n}_i \\ &= \lambda_i(t) (\mathbf{v}_i - \mathbf{v}_q)^T \mathbf{n}_i = \lambda_i(t) \text{dist}(\mathbf{v}_i, \pi_i) \end{aligned}$$

which implies that:

$$\lambda_i(t) = \frac{\text{dist}(\mathbf{p}(t), \pi_i)}{\text{dist}(\mathbf{v}_i, \pi_i)} \quad (2)$$

Hence, $\lambda_i(t)$ represents the ratio between the distance from the point $\mathbf{p}(t)$ of the curve to the hyperplane π_i and the distance from \mathbf{v}_i to that hyperplane π_i (see Fig. 2 for the case $n = 3$)¹. From Eq. 2 it is clear that each $\lambda_i(t)$ is an n^{th} -degree polynomial, that we will write as $\lambda_i(t) := \boldsymbol{\lambda}_i^T \mathbf{t}$, where $\boldsymbol{\lambda}_i$ is its vector of coefficients. Matching

¹Note that multiplying numerator and denominator of Eq. 2 by the area of the facet that lies on the plane π_i , each $\lambda_i(t)$ can also be defined as a ratio of volumes, as in [Ericson 2004]

now the coefficients of $\mathbf{p}(t)$ with the ones of $\sum_{i=0}^n \lambda_i(t) \mathbf{v}_i$, the first constraint of Eq. 1 can be rewritten as:

$$\mathbf{P} = \mathbf{V} \underbrace{\begin{bmatrix} \lambda_0^T \\ \lambda_1^T \\ \vdots \\ \lambda_n^T \end{bmatrix}}_{:=\mathbf{A}}$$

where we have also defined the $(n+1) \times (n+1)$ matrix \mathbf{A} , whose i -th row contains the coefficients of the polynomial $\lambda_i(t)$ in decreasing order. The second and third constraints of Eq. 1 can be rewritten as $\mathbf{A}^T \mathbf{1} = \mathbf{e}$ and $\mathbf{A} \mathbf{t} \geq \mathbf{0} \ \forall t \in [-1, 1]$ respectively. We conclude therefore that

$$\mathbf{P} \subset S \equiv \left\{ \begin{array}{l} \mathbf{P} = \mathbf{V} \mathbf{A} \\ \mathbf{A}^T \mathbf{1} = \mathbf{e} \\ \mathbf{A} \mathbf{t} \geq \mathbf{0} \ \forall t \in [-1, 1] \end{array} \right\} \quad (3)$$

5.2 Objective Function of Problem 1

Using the constraints in Eq. 3, and noting that the matrix \mathbf{A} is invertible (as proven in the Appendix, Section B), we can write

$$f_1 \propto \text{abs} \left(\left\| \begin{bmatrix} \mathbf{V}^T & \mathbf{1} \end{bmatrix} \right\| \right) = \text{abs} \left(\left\| \mathbf{A}^{-T} \begin{bmatrix} \mathbf{P}^T & \mathbf{e} \end{bmatrix} \right\| \right) \propto \text{abs} \left(\left\| \mathbf{A}^{-1} \right\| \right) = \frac{1}{\text{abs}(|\mathbf{A}|)}$$

where we have used the fact that everything inside $\begin{bmatrix} \mathbf{P}^T & \mathbf{e} \end{bmatrix}$ is given (i.e., not a decision variable of the optimization problem), and the fact that $|\mathbf{A}| = |\mathbf{A}^T|$. We can therefore maximize $\text{abs}(|\mathbf{A}|)$, or, equivalently, minimize $-\text{abs}(|\mathbf{A}|)$. Note that now the objective function f_1 is **independent** of the curve \mathbf{P} given.

5.3 Objective Function of Problem 2

Similar to the previous subsection, and noting that \mathbf{V} is given in Problem 2, we have that

$$f_2 \propto -\text{abs} \left(\left\| \begin{bmatrix} \mathbf{P} \\ \mathbf{e}^T \end{bmatrix} \right\| \right) = -\text{abs} \left(\left\| \begin{bmatrix} \mathbf{V} \\ \mathbf{1}^T \end{bmatrix} \mathbf{A} \right\| \right) \propto -\text{abs}(|\mathbf{A}|)$$

and therefore the objective function f_2 is now **independent** of the simplex S given.

5.4 Equivalent Formulation for Problem 1 and 2

Note that now the dependence on the polynomial curve given (for Problem 1) or on the simplex given (for Problem 2) appears only in the constraint $\mathbf{P} = \mathbf{V} \mathbf{A}$. As \mathbf{A} is invertible, we can safely remove this constraint from the optimization, leaving \mathbf{A} as the only decision variable, and then use $\mathbf{P} = \mathbf{V} \mathbf{A}$ to obtain \mathbf{V} (for Problem 1) or \mathbf{P} (for Problem 2). We end up therefore with the following optimization problem²:

²Note that in the objective function of Problem 3 the $\text{abs}(\cdot)$ is not necessary, since any permutation of the rows of \mathbf{A} will change the sign of $|\mathbf{A}|$. We keep it simply for consistency purposes, since later in the solutions we will show a specific order of the rows of \mathbf{A} for which (for some n) $|\mathbf{A}| < 0$, but that allows us to highlight the similarities and differences between this matrix and the ones Bernstein and B-Spline bases use.

Problem 3:

$$\begin{array}{ll} \min_{\mathbf{A} \in \mathbb{R}^{(n+1) \times (n+1)}} & f_3 := -\text{abs}(|\mathbf{A}|) \\ \text{s.t.} & \mathbf{A}^T \mathbf{1} = \mathbf{e} \\ & \mathbf{A} \mathbf{t} \geq \mathbf{0} \ \forall t \in [-1, 1] \end{array}$$

Remark. As detailed above, Problem 3 does not depend on the specific n^{th} -order polynomial curve given (for Problem 1) or on the specific n -simplex given (for Problem 2). Hence, its optimal solution \mathbf{A}^* for a specific n can be applied to obtain the optimal solution of Problem 1 for **any** given polynomial curve $\mathbf{P} \in \mathcal{P}^n$ (by using $\mathbf{V}^* = \mathbf{P} (\mathbf{A}^*)^{-1}$) and to obtain the optimal solution of Problem 2 for **any** given simplex $S \in \mathcal{S}^n$ (by using $\mathbf{P}^* = \mathbf{V} \mathbf{A}^*$)

As the objective function of Problem 3 is the determinant of the nonsymmetric matrix \mathbf{A} , it is clearly a nonconvex problem. We can rewrite the constraint $\mathbf{A} \mathbf{t} \geq \mathbf{0} \ \forall t \in [-1, 1]$ of Problem 3 using Sum-Of-Squares programming [Parrilo 2006]:

- If n is odd, $\lambda_i(t) \geq 0 \ \forall t \in [-1, 1]$ if and only if

$$\begin{cases} \lambda_i(t) = \hat{\mathbf{t}}^T ((t+1)\mathbf{W}_i + (1-t)\mathbf{V}_i) \hat{\mathbf{t}} \\ \mathbf{W}_i \in \mathbb{S}_+^{\frac{n+1}{2}}, \mathbf{V}_i \in \mathbb{S}_+^{\frac{n+1}{2}} \end{cases}$$

- If n is even, $\lambda_i(t) \geq 0 \ \forall t \in [-1, 1]$ if and only if

$$\begin{cases} \lambda_i(t) = \hat{\mathbf{t}}^T \mathbf{W}_i \hat{\mathbf{t}} + \hat{\mathbf{t}}^T (t+1)(1-t)\mathbf{V}_i \hat{\mathbf{t}} \\ \mathbf{W}_i \in \mathbb{S}_+^{\frac{n}{2}+1}, \mathbf{V}_i \in \mathbb{S}_+^{\frac{n}{2}} \end{cases}$$

Note that the *if and only if* condition applies because $\lambda_i(t)$ is a univariate polynomial [Parrilo 2006]. The decisions variables would be the positive semidefinite matrices \mathbf{W}_i and \mathbf{V}_i , $i = 0, \dots, n$. Other option is to use the Markov–Lukács theorem ([Szeg 1939, Theorem 1.21.1], [Krein et al. 1977, Theorem 2.2], [Roh and Vandenberghe 2006]):

- If n is odd, $\lambda_i(t) \geq 0 \ \forall t \in [-1, 1]$ if and only if

$$\lambda_i(t) = (t+1)g_i^2(t) + (1-t)h_i^2(t)$$

- If n is even, $\lambda_i(t) \geq 0 \ \forall t \in [-1, 1]$ if and only if

$$\lambda_i(t) = g_i^2(t) + (t+1)(1-t)h_i^2(t)$$

where $g_i(t)$ and $h_i(t)$ are polynomials of degrees $\deg(g_i(t)) \leq \lfloor n/2 \rfloor$ and $\deg(h_i(t)) \leq \lfloor (n-1)/2 \rfloor$. The decision variables would be the coefficients of the polynomials $g_i(t)$ and $h_i(t)$, $i = 0, \dots, n$. In Appendix C we derive the Karush–Kuhn–Tucker (KKT) conditions of Problem 3 using this theorem.

Regardless of the choice of the representation of the constraint $\mathbf{A} \mathbf{t} \geq \mathbf{0} \ \forall t \in [-1, 1]$ (SOS or the Markov–Lukács theorem), no generality has been lost so far. However, these formulations easily become intractable for large n due to the high number of decision variables. We can reduce the number of decision variables of Problem 3 by imposing a structure in $\lambda_i(t)$. As Problem 1 is trying to minimize the volume of the simplex, we can impose that the facets of the n -simplex be tangent to some internal points $\mathbf{p}(t)$ of the curve (with $t \in (-1, 1)$), and in contact with the first and last points of the curve ($\mathbf{p}(-1)$ and $\mathbf{p}(1)$) [Klee 1986; Zhou and Suri 2002]. Using the geometric interpretation of the $\lambda_i(t)$ given in Section 5.1, this means that each $\lambda_i(t)$ should have either real double roots in $t \in (-1, 1)$ (where the curve is tangent to a facet), and/or roots at $t = \{-1, 1\}$.

Problem 4:

$$\min_{A \in \mathbb{R}^{(n+1) \times (n+1)}} f_4 := -\text{abs}(|A|)$$

s.t. :

If n is odd:

$$\begin{aligned} \lambda_i(t) &= -b_i(t-1) \prod_{j=1}^{\frac{n-1}{2}} (t-t_{ij})^2 & i = 0, 2, \dots, n-1 \\ \lambda_i(t) &= \lambda_{n-i}(-t) & i = 1, 3, \dots, n \\ b_i &\geq 0 & i = 0, 2, \dots, n-1 \\ A^T \mathbf{1} &= \mathbf{e} \end{aligned}$$

If n is even: define \mathcal{I}_a the set of odd integers $\in [0, \frac{n}{2} - 1]$, and \mathcal{I}_b the set of even integers $\in [0, \frac{n}{2} - 1]$:

$$\begin{aligned} \lambda_i(t) &= -b_i(t+1)(t-1) \prod_{j=1}^{\frac{n-2}{2}} (t-t_{ij})^2 & i \in \mathcal{I}_a \\ \lambda_i(t) &= b_i \prod_{j=1}^{\frac{n}{2}} (t-t_{ij})^2 & i \in \mathcal{I}_b \\ \lambda_i(t) &= \lambda_{n-i}(-t) & i = \frac{n}{2} + 1, \dots, n \\ b_i &\geq 0 & i = 0, 1, \dots, \frac{n}{2} \\ A^T \mathbf{1} &= \mathbf{e} \end{aligned}$$

- If $\frac{n}{2}$ is odd ($n = 2, 6, 10, \dots$):

$$\lambda_i(t) = -b_i(t+1)(t-1) \prod_{j=1}^{\frac{n-2}{4}} (t-t_{ij})^2 (t+t_{ij})^2 \quad i = \frac{n}{2}$$

- If $\frac{n}{2}$ is even ($n = 4, 8, 12, \dots$):

$$\lambda_i(t) = b_i \prod_{j=1}^{\frac{n}{4}} (t-t_{ij})^2 (t+t_{ij})^2 \quad i = \frac{n}{2}$$

These conditions, together with an additional symmetry condition between different $\lambda_i(t)$, translate into the formulation shown in Problem 4, in which the decisions variables are the roots of $\lambda_i(t)$ and the coefficients b_i .

The relationship between Problems 1, 2, 3 and 4 is given in Fig. 3. First note that the structure imposed for $\lambda_i(t)$ in Problem 4 guarantees that they are nonnegative for $t \in [-1, 1]$. Hence the feasible set of Problem 4 is contained in the feasible set of Problem 3, and therefore, $f_3^* \leq f_4^*$ holds. The matrix A found in Problem 3 or 4 can be used to find the vertexes of the simplex in Problem 1 (by simply using $V = P(A)^{-1}$, where P is the coefficient matrix of the polynomial curve given), or to find the coefficient matrix of the polynomial curve in Problem 2 (by using $P = VA$, where V contains the vertexes of the simplex given).

6 RESULTS

Using the nonconvex solvers *fmincon* [MATLAB Optimization Toolbox 2020] and *SNOPT* [Gill et al. 2005, 2018] (with the *YALMIP* interface [Löfberg 2004, 2009]), we were able to find local minima for Problem 4 for $n = 1, 2, \dots, 7$, and the same local minima were found in Problem 3 for $n = 1, 2, 3, 4$. Problem 3 and 4 become intractable for $n \geq 5$ and $n \geq 8$ respectively. The optimal matrices A

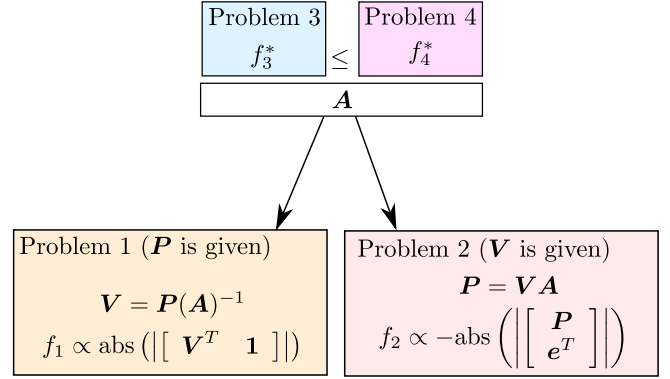


Fig. 3. Relationship between Problems 1, 2, 3 and 4: Problem 3 and 4 have the same objective function, but the feasible set of Problem 4 is contained in the feasible set of Problem 3, and therefore $f_3^* \leq f_4^*$. Both Problem 3 and 4 generate a solution A , which can be applied to **any** polynomial curve $P \in \mathcal{P}^n$ to find the simplex $S \in \mathcal{S}^n$ in Problem 1, or to **any** simplex $S \in \mathcal{S}^n$ to find the polynomial curve $P \in \mathcal{P}^n$ in Problem 2.

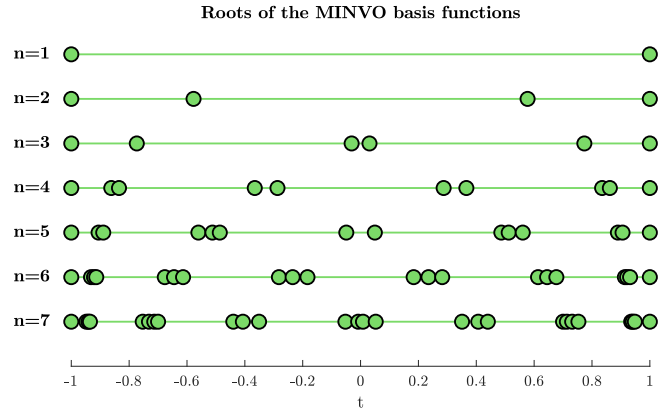


Fig. 4. Distribution of the roots of the MINVO basis functions for different n . These roots are also available in Table 3.

found are shown in Table 2, and denoted as A_{MV}^3 . Its determinant $|A_{MV}|$ is also compared with the one of the Bernstein and B-Spline matrices (denoted as A_{Be} and A_{Bs} respectively). The corresponding plots of the MINVO basis functions are shown in Fig. 6, together with the Bernstein, B-Spline and Lagrange bases for comparison. All these bases satisfy $\sum_{i=0}^n \lambda_i(t) = 1$, and the MINVO, Bernstein and B-Spline bases also satisfy $\lambda_i(t) \geq 0 \quad \forall t \in [-1, 1]$. The roots of each of the MINVO basis functions $\lambda_i(t)$ are shown in Table 3 and plotted in Fig. 4.

One natural question to ask is whether the basis found constitutes a global minimizer for either Problem 3 or Problem 4. To answer this, first note that both Problem 3 and Problem 4 are polynomial optimization problems. Therefore, we can make use of Lasserre's moment method [Lasserre 2001], and increase the order of the moment relaxation to find tighter lower bounds of the original nonconvex polynomial optimization problem. Using this technique, we were

³Note that any permutation in the rows of A_{MV} will not change the objective value, since only the sign of the determinant is affected.

Table 2. Results for the MINVO basis. A_{MV} , A_{Be} and A_{BS} denote the coefficient matrix of the MINVO, Bernstein and B-Spline bases respectively ($t \in [-1, 1]$). The greater the absolute value of the determinant, the smaller the associated simplex (for Problem 1) and the larger the convex hull of the curve (for Problem 2). The matrices A_{MV} found are **independent** of the polynomial curve given (in Problem 1), or of the simplex given (in Problem 2).

n	A_{MV}	$\text{abs}(A_{MV})$	$\frac{\text{abs}(A_{MV})}{\text{abs}(A_{Be})}$	$\frac{\text{abs}(A_{MV})}{\text{abs}(A_{BS})}$	Problem 3	Problem 4
1	$\begin{bmatrix} \frac{1}{2} & -1 & 1 \\ 1 & 1 & 1 \end{bmatrix}$	$\frac{1}{2} = 0.5$	$= 1$	$= 1$	Global Opt.	Global Opt.
2	$\frac{1}{8} \begin{bmatrix} 3 & -2\sqrt{3} & 1 \\ -6 & 0 & 6 \\ 3 & 2\sqrt{3} & 1 \end{bmatrix}$	$\frac{3\sqrt{3}}{16} \approx 0.3248$	≈ 1.299	≈ 5.196	Global Opt.	Global Opt.
3	$\begin{bmatrix} -0.4302 & 0.4568 & -0.02698 & 0.0004103 \\ 0.8349 & -0.4568 & -0.7921 & 0.4996 \\ -0.8349 & -0.4568 & 0.7921 & 0.4996 \\ 0.4302 & 0.4568 & 0.02698 & 0.0004103 \end{bmatrix}$	≈ 0.3319	≈ 2.360	≈ 254.9	Global Opt.	Global Opt.
4	$\begin{bmatrix} 0.5255 & -0.5758 & -0.09435 & 0.1381 & 0.03023 \\ -1.108 & 0.8108 & 0.9602 & -0.8108 & 0.1483 \\ 1.166 & 0 & -1.732 & 0 & 0.643 \\ -1.108 & -0.8108 & 0.9602 & 0.8108 & 0.1483 \\ 0.5255 & 0.5758 & -0.09435 & -0.1381 & 0.03023 \end{bmatrix}$	≈ 0.5678	≈ 6.057	$\approx 1.675 \cdot 10^5$	Local Opt. (at least)	Local Opt. (at least)
5	$\begin{bmatrix} -0.7392 & 0.7769 & 0.3302 & -0.3773 & -0.0365 & 0.04589 \\ 1.503 & -1.319 & -1.366 & 1.333 & -0.121 & 0.002895 \\ -1.75 & 0.5424 & 2.777 & -0.9557 & -1.064 & 0.4512 \\ 1.75 & 0.5424 & -2.777 & -0.9557 & 1.064 & 0.4512 \\ -1.503 & -1.319 & 1.366 & 1.333 & 0.121 & 0.002895 \\ 0.7392 & 0.7769 & -0.3302 & -0.3773 & 0.0365 & 0.04589 \end{bmatrix}$	≈ 1.6987	≈ 22.27	$\approx 1.924 \cdot 10^9$	Feasible (at least)	Local Opt. (at least)
6	$\begin{bmatrix} 1.06 & -1.134 & -0.7357 & 0.8348 & 0.1053 & -0.1368 & 0.01836 \\ -2.227 & 2.055 & 2.281 & -2.299 & -0.08426 & 0.2433 & 0.0312 \\ 2.59 & -1.408 & -4.27 & 2.468 & 1.58 & -1.081 & 0.152 \\ -2.844 & 0 & 5.45 & 0 & -3.203 & 0 & 0.5969 \\ 2.59 & 1.408 & -4.27 & -2.468 & 1.58 & 1.081 & 0.152 \\ -2.227 & -2.055 & 2.281 & 2.299 & -0.08426 & -0.2433 & 0.0312 \\ 1.06 & 1.134 & -0.7357 & -0.8348 & 0.1053 & 0.1368 & 0.01836 \end{bmatrix}$	≈ 9.1027	≈ 117.8	$\approx 4.750 \cdot 10^{14}$	Feasible (at least)	Local Opt. (at least)
7	$\begin{bmatrix} -1.637 & 1.707 & 1.563 & -1.682 & -0.3586 & 0.4143 & -0.006851 & 2.854 \cdot 10^{-5} \\ 3.343 & -3.285 & -3.947 & 4.173 & 0.6343 & -0.9385 & -0.02111 & 0.05961 \\ -4.053 & 2.722 & 6.935 & -4.96 & -2.706 & 2.269 & -0.2129 & 0.00535 \\ 4.478 & -1.144 & -9.462 & 2.469 & 6.311 & -1.745 & -1.312 & 0.435 \\ -4.478 & -1.144 & 9.462 & 2.469 & -6.311 & -1.745 & 1.312 & 0.435 \\ 4.053 & 2.722 & -6.935 & -4.96 & 2.706 & 2.269 & 0.2129 & 0.00535 \\ -3.343 & -3.285 & 3.947 & 4.173 & -0.6343 & -0.9385 & 0.02111 & 0.05961 \\ 1.637 & 1.707 & -1.563 & -1.682 & 0.3586 & 0.4143 & 0.006851 & 2.854 \cdot 10^{-5} \end{bmatrix}$	≈ 89.0191	≈ 902.7	$\approx 2.997 \cdot 10^{21}$	Feasible (at least)	Local Opt. (at least)

able to obtain the same objective value (proving therefore global optimality) for $n = 1, 2, 3$ in Problem 4. For Problem 3, the moment relaxation technique becomes intractable due to the high number of variables. Hence, to prove global optimality in Problem 3 we use instead the branch-and-bound algorithm, which proves global optimality by reducing to zero the gap between the upper bounds found by a nonconvex solver, and the lower bounds found using convex relaxations [Löfberg 2020]. This technique proved to be tractable for cases $n = 1, 2, 3$ in Problem 3, and zero optimality gap was obtained.

All these results lead us to the following conclusions, which are also summarized in Table 2:

- The matrices A_{MV} found for $n = 1, 2, 3$ are global minimizers of both Problem 3 and Problem 4.
- The matrix A_{MV} found for $n = 4$ is at least a local minimizer of both Problem 3 and Problem 4.
- The matrices A_{MV} found for $n = 5, 6, 7$ are at least local minimizers for Problem 4, and are at least feasible solutions for Problem 3.

Here we have classified as local optima the solutions found by the numerical solver for which the first-order optimality measure and the maximum constraint violation are smaller than a predefined small tolerance [MATLAB Optimization Toolbox 2020].

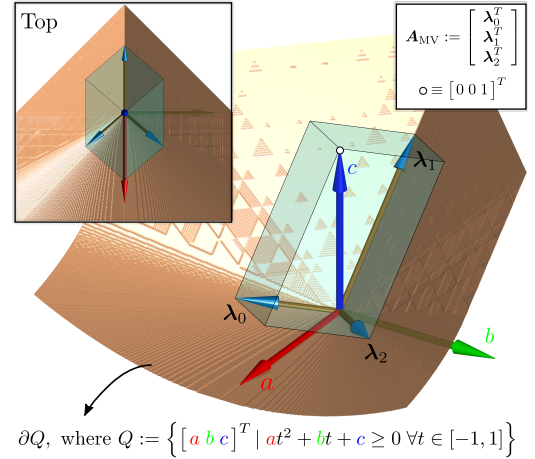


Fig. 5. For $n = 2$, the MINVO basis has $A_{MV} = [\lambda_0 \ \lambda_1 \ \lambda_2]^T$, where λ_0, λ_1 and λ_2 are vectors that span the blue parallelepiped, and whose sum is $[0 \ 0 \ 1]^T$. The frontier of the cone formed by the coefficients of the polynomials that are nonnegative $\forall t \in [-1, 1]$ is shown in orange. Note how the globally-optimal vectors λ_0, λ_1 and λ_2 belong to this frontier.

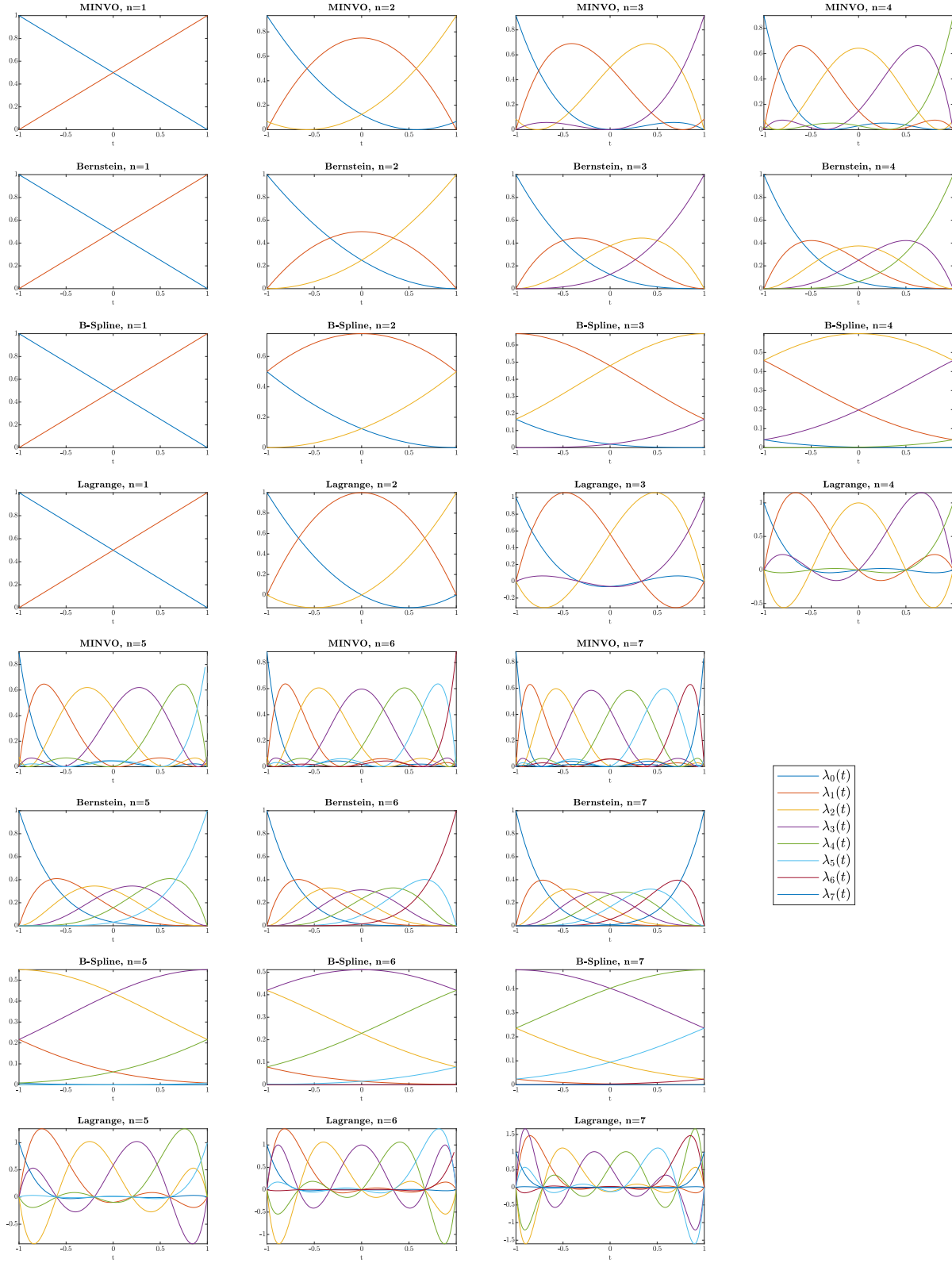


Fig. 6. Comparison between the MINVO, Bernstein, B-Spline, and Lagrange bases for $n = 1, 2, \dots, 7$. All these bases satisfy $\sum_{i=0}^n \lambda_i(t) = 1$, and the MINVO, Bernstein and B-Spline bases also satisfy $\lambda_i(t) \geq 0 \quad \forall t \in [-1, 1]$.

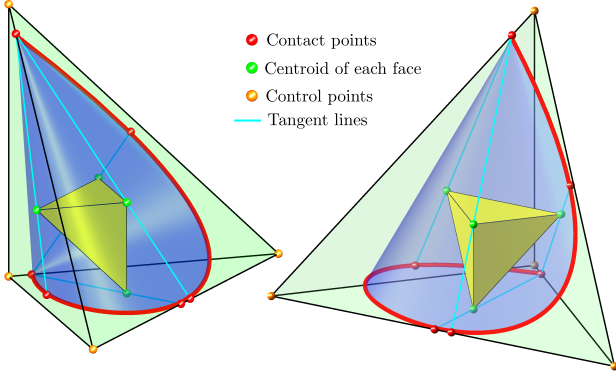
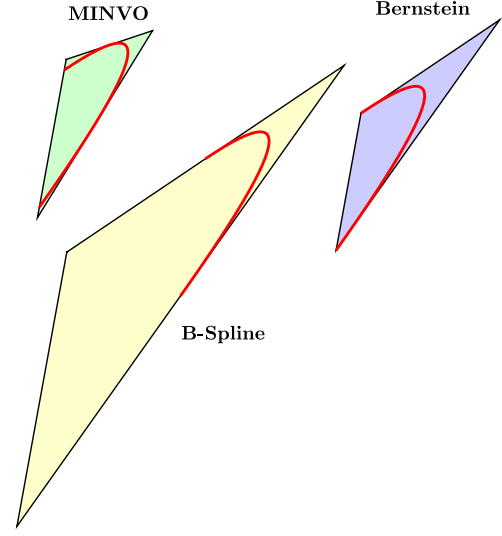


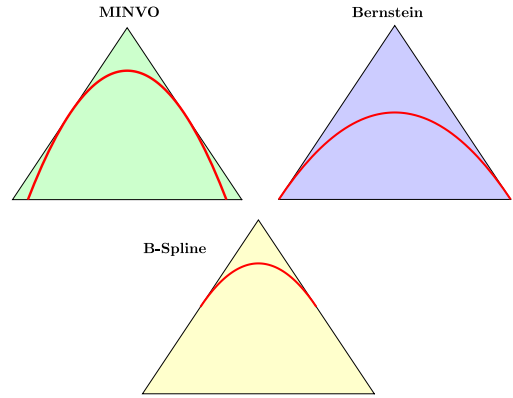
Fig. 7. Solution obtained by the MINVO basis for $n = 3$. Note how the centroids of each of the faces (green points) belong to $\text{conv}(P)$, which is a necessary condition for local optimality [Klee 1986]. Moreover, note that $\text{conv}(P)$ is tangent to the simplex along the blue lines. The red points denote the contact points between the curve and the simplex, which happen at the roots of the MINVO basis functions. The yellow tetrahedron has its vertexes on the centroids of the faces, and it is completely contained in $\text{conv}(P)$.

Table 3. Roots of each $\lambda_i(t)$ of the MINVO basis. $\mathbf{r}(\lambda_i(t))$ is the column vector that contains the roots of $\lambda_i(t)$. All the roots $\in (-1, 1)$ are double roots, while the ones $\in \{-1, 1\}$ are single roots. Each $\lambda_i(t)$ has n real roots in total. These roots are plotted in Fig. 4.

n	Roots of $\lambda_i(t)$, $t \in [-1, 1]$				
1	$\begin{bmatrix} r(\lambda_0)^T \\ r(\lambda_1)^T \end{bmatrix}$	=	$\begin{bmatrix} 1.0 \\ -1.0 \end{bmatrix}$		
2	$\begin{bmatrix} r(\lambda_0)^T \\ r(\lambda_1)^T \\ r(\lambda_2)^T \end{bmatrix}$	=	$\begin{bmatrix} \frac{1}{\sqrt{3}} \\ -1.0 \\ -\frac{1}{\sqrt{3}} \end{bmatrix}$	1.0	
3	$\begin{bmatrix} r(\lambda_0)^T \\ r(\lambda_1)^T \\ r(\lambda_2)^T \\ r(\lambda_3)^T \end{bmatrix}$	\approx	$\begin{bmatrix} 0.03088 & 1.0 \\ -1.0 & 0.7735 \\ -0.7735 & 1.0 \\ -1.0 & -0.03088 \end{bmatrix}$		
4	$\begin{bmatrix} r(\lambda_0)^T \\ r(\lambda_1)^T \\ r(\lambda_2)^T \\ r(\lambda_3)^T \\ r(\lambda_4)^T \end{bmatrix}$	\approx	$\begin{bmatrix} -0.2872 & 0.835 \\ -1.0 & 0.3657 \\ -0.8618 & 0.8618 \\ -1.0 & -0.3657 \\ -0.835 & 0.2872 \end{bmatrix}$	1.0	
5	$\begin{bmatrix} r(\lambda_0)^T \\ r(\lambda_1)^T \\ r(\lambda_2)^T \\ r(\lambda_3)^T \\ r(\lambda_4)^T \\ r(\lambda_5)^T \end{bmatrix}$	\approx	$\begin{bmatrix} -0.4866 & 0.5121 & 1.0 \\ -1.0 & 0.04934 & 0.8895 \\ -0.9057 & 0.5606 & 1.0 \\ -1.0 & -0.5606 & 0.9057 \\ -0.8895 & -0.04934 & 1.0 \\ -1.0 & -0.5121 & 0.4866 \end{bmatrix}$		
6	$\begin{bmatrix} r(\lambda_0)^T \\ r(\lambda_1)^T \\ r(\lambda_2)^T \\ r(\lambda_3)^T \\ r(\lambda_4)^T \\ r(\lambda_5)^T \\ r(\lambda_6)^T \end{bmatrix}$	\approx	$\begin{bmatrix} -0.6135 & 0.2348 & 0.9137 \\ -1.0 & -0.1835 & 0.6449 \\ -0.9317 & 0.2822 & 0.9214 \\ -1.0 & -0.6768 & 0.6768 \\ -0.9214 & -0.2822 & 0.9317 \\ -1.0 & -0.6449 & 0.1835 \\ -0.9137 & -0.2348 & 0.6135 \end{bmatrix}$	1.0	
7	$\begin{bmatrix} r(\lambda_0)^T \\ r(\lambda_1)^T \\ r(\lambda_2)^T \\ r(\lambda_3)^T \\ r(\lambda_4)^T \\ r(\lambda_5)^T \\ r(\lambda_6)^T \\ r(\lambda_7)^T \end{bmatrix}$	\approx	$\begin{bmatrix} -0.7 & 0.008364 & 0.7132 & 1.0 \\ -1.0 & -0.3509 & 0.4068 & 0.9355 \\ -0.9481 & 0.05239 & 0.7315 & 1.0 \\ -1.0 & -0.753 & 0.4399 & 0.9408 \\ -0.9408 & -0.4399 & 0.753 & 1.0 \\ -1.0 & -0.7315 & -0.05239 & 0.9481 \\ -0.9355 & -0.4068 & 0.3509 & 1.0 \\ -1.0 & -0.7132 & -0.008364 & 0.7 \end{bmatrix}$		



(a) For any given curve $P \in \mathcal{P}^2$, the MINVO basis finds an enclosing 2-simplex that is ≈ 1.3 and ≈ 5.2 times smaller than the one found by the Bernstein and B-Spline bases respectively.

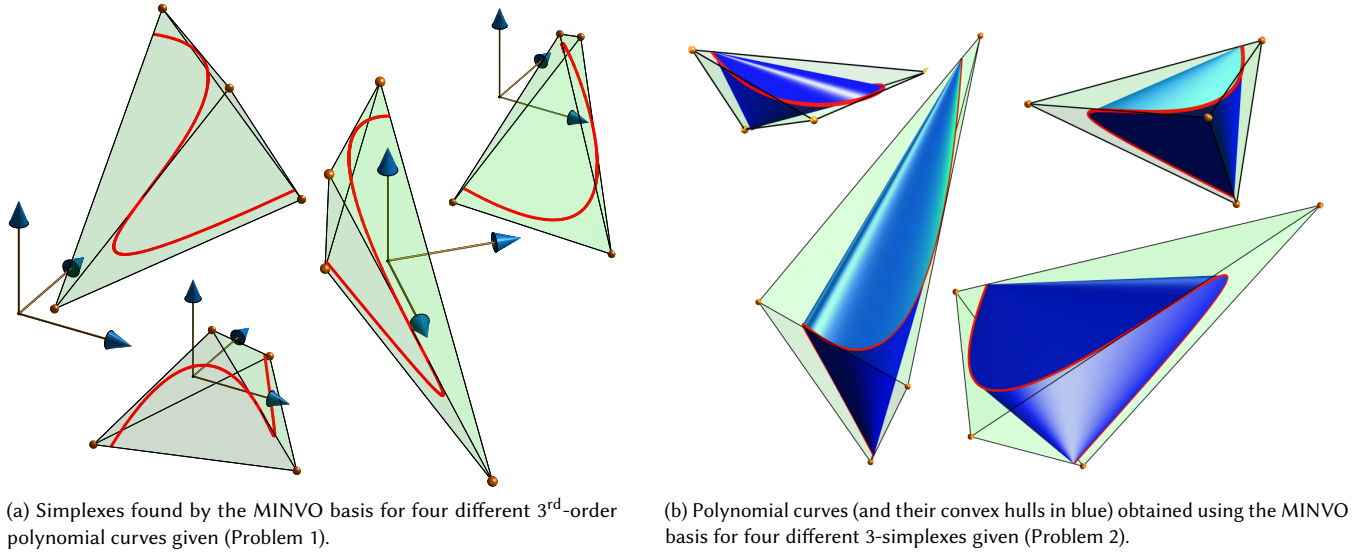


(b) For any given 2-simplex, the MINVO basis finds a curve $P \in \mathcal{P}^2$ inscribed in the simplex, and whose convex hull is ≈ 1.3 and ≈ 5.2 times larger than the one found by the Bernstein and B-Spline bases respectively.

Fig. 8. Comparison between the MINVO, Bernstein and B-Spline bases for $n = 2$. The MINVO basis obtains globally optimal results for $n = 1, 2, 3$.

The geometric interpretation of Problem 3 (for $n = 2$) is shown in Fig. 5. The rows of \mathbf{A} are vectors that lie in the cone of the polynomials that are nonnegative in $t \in [-1, 1]$ (and whose frontier is shown in orange in the figure). As Problem 3 is maximizing the volume of the parallelepiped spanned by these vectors, the optimal minimizer is obtained in the frontier of the cone, while guaranteeing that the sum of these vectors is $[0 \ 0 \ 1]^T$.

In Fig. 7 we check that the centroids of each of the faces of the simplex belongs to $\text{conv}(P)$, which is a necessary condition for

Fig. 9. MINVO results for $n = 3$, where global optimality is guaranteed.

that simplex to be minimal [Klee 1986]. Note also that $\text{conv}(P)$ is tangent to the simplex along four lines (in blue in the figure), and that the contact points of the curve with the simplex happen at the roots of the MINVO basis functions.

When the polynomial curve is given (i.e., Problem 1), the ratio between the volume of the simplex S_α obtained by a basis α and the volume of the simplex S_β obtained by a basis β ($\alpha, \beta \in \{\text{MV}, \text{Be}, \text{BS}\}$) is given by

$$\frac{\text{vol}(S_\alpha)}{\text{vol}(S_\beta)} = \frac{\text{abs}(|A_\beta|)}{\text{abs}(|A_\alpha|)}$$

Similarly, when the simplex is given (i.e., Problem 2), the ratio between the volume of the convex hull of the polynomial curve P_α found by a basis α and the volume of the convex hull of the polynomial curve P_β found by a basis β ($\alpha, \beta \in \{\text{MV}, \text{Be}, \text{BS}\}$) is given by

$$\frac{\text{vol}(\text{conv}(P_\alpha))}{\text{vol}(\text{conv}(P_\beta))} = \frac{\text{abs}(|A_\alpha|)}{\text{abs}(|A_\beta|)}$$

These ratios are shown in Table 2, and they mean the following for Problem 1 (Problem 2 respectively):

- For $n = 3$, the MINVO basis finds a simplex that has a volume (a polynomial curve whose convex hull has a volume) ≈ 2.36 and ≈ 254.9 times smaller (larger) than the one the Bernstein and B-Spline bases find respectively.
- For $n = 7$, the MINVO basis finds a simplex that has a volume (a polynomial curve whose convex hull has a volume) ≈ 902.7 and $\approx 2.997 \cdot 10^{21}$ times smaller (larger) than the one the Bernstein and B-Spline bases find respectively.

An analogous reasoning applies to the volume ratios of other n . These comparisons are shown in Fig. 8 (for $n = 2$), and in Fig. 1 (for $n = 3$). More examples of the MINVO bases applied to different polynomial curves and simplexes are shown in Fig. 9.

7 MINVO BASIS APPLIED TO OTHER CURVES AND SURFACES

7.1 Polynomial curves of degree n , dimension k , and embedded in a subspace \mathcal{M} of dimension m

So far we have studied the case of $n = m = k$ (i.e., a polynomial curve of degree n and dimension $k = n$ and for which n is also the dimension of \mathcal{M} , see Section 3.1). The most general case would be any k, n and m , as shown in Table 4. In all these cases, and using the $(n+1) \times (n+1)$ matrix A_{MV} , we can still apply the equation $V_{k \times (n+1)} = P_{k \times (n+1)} A_{\text{MV}}^{-1}$ to obtain all the $n+1$ MINVO control points $\in \mathbb{R}^k$ of the given curve (columns of the matrix V). The convex hull of the control points is guaranteed to contain the curve

		Degree n						
		1	2	3	4	5	6	7
Dimension k	1	G	F	F	F	F	F	F
	2	G	G	F	F	F	F	F
	3	G	G	G	F	F	F	F
	4	G	G	G	L	F	F	F
	5	G	G	G	L	F	F	F
	6	G	G	G	L	F	F	F
	7	G	G	G	L	F	F	F
<p>In all the cases (and for any m): there are $n+1$ control points, and $\text{conv}(\text{control points})$ is a polyhedron $\subset \mathcal{M} \subseteq \mathbb{R}^k$ that encloses the curve and that has at most $n+1$ vertices.</p> <p>In and below the diagonal: When $n = m$, the polyhedron is a simplex that is at least globally-optimal (G), locally-optimal (L), or feasible (F).</p>								

Table 4. All the possible cases of polynomial curves of degree n , dimension k , and embedded in a subspace \mathcal{M} of dimension m . Note that $m \leq \min(k, n)$ always holds.

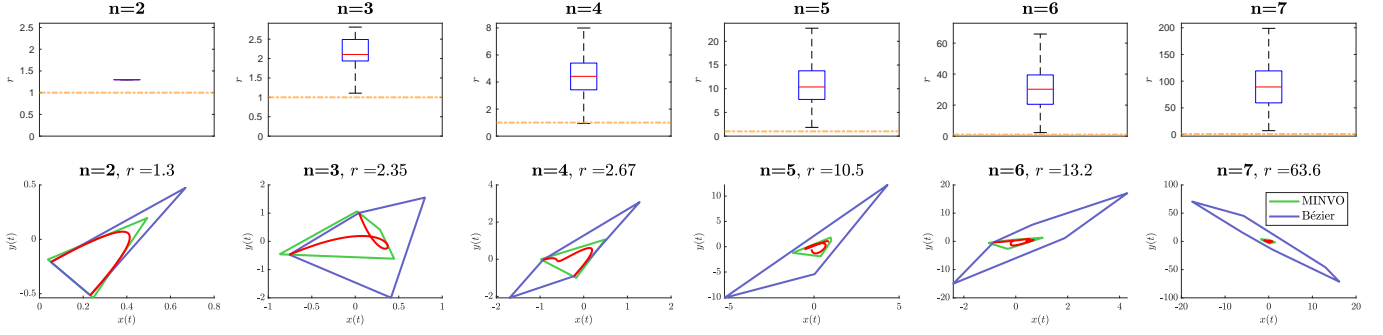


Fig. 10. Comparison of the convex hull of the MINVO and Bézier control points for $k = m = 2$ and different n . Here r denotes the ratio of the areas $\frac{A_{Be}}{A_{MV}}$. The boxplots (top) have been obtained from 10^4 polynomials passing through $n + 1$ random points in the square $[-1, 1]^2$. The yellow dashed line highlights the value $r = \frac{A_{Be}}{A_{MV}} = 1$. Some of these random curves and the associated convex hulls are shown at the bottom.

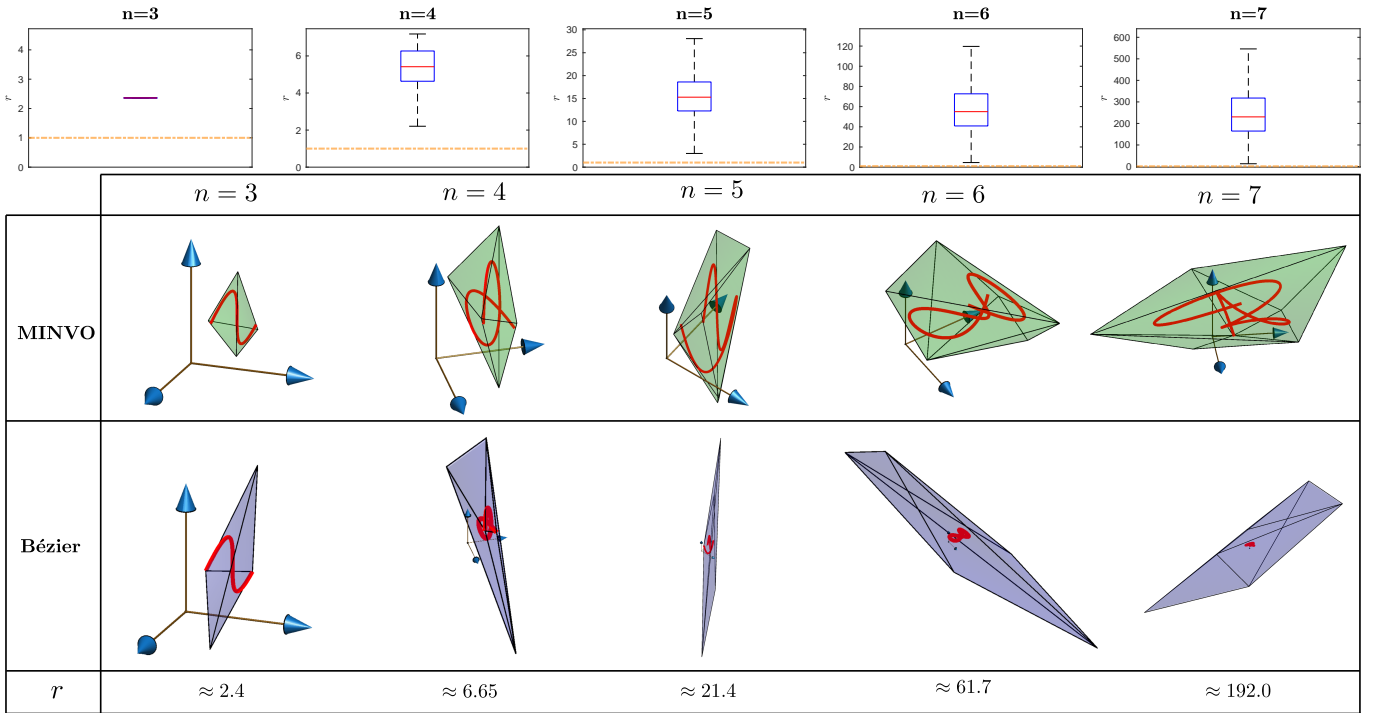


Fig. 11. Comparison of the convex hull of the MINVO and Bézier control points for $k = m = 3$ and different n . Here r denotes the ratio of the volumes $\frac{V_{Be}}{V_{MV}}$. The boxplots (top) have been obtained from 10^4 polynomials passing through $n + 1$ random points in the cube $[-1, 1]^3$ were used. The yellow dashed line highlights the value $r = \frac{V_{Be}}{V_{MV}} = 1$. Some of these random curves and the associated convex hulls are shown at the bottom.

because the curve is a convex combination of the control points. Note also that, when $n = m$, all the cases below the diagonal of Table 4 have the same optimality properties (global/local/feasible) as the diagonal element that has the same n .

For $k = 3$, different combinations of m and n are shown in Fig. 13: A cubic curve embedded in a two-dimensional subspace, a segment embedded in a one-dimensional subspace and a quadratic curve embedded in a two-dimensional subspace.

For $k = m = 2$, the comparison between the area of the convex hull of the MINVO control points (A_{MV}) and the area of the convex hull of the Bézier control points (A_{Be}) is shown in Fig. 10. Note that

this ratio is constant for any polynomial curve for the case $n = 2$, but depends on the curve given for the cases $n > 2$. To generate the boxplots of Fig. 10, we used a total of 10^4 polynomials passing through $n + 1$ points randomly sampled from the square $[-1, 1]^2$. Although it is not guaranteed that $A_{MV} < A_{Be}$ for any polynomial with $n > 2$, the Monte Carlo analysis performed using these random polynomials shows that $A_{MV} < A_{Be}$ holds for the great majority of them, with improvements up to ≈ 200 times for the case $n = 7$.

Similarly, the results for $k = m = 3$ are shown in Fig. 11, where we used a total of 10^4 polynomials passing through $n + 1$ points randomly sampled from the cube $[-1, 1]^3$. Again, it is not guaranteed

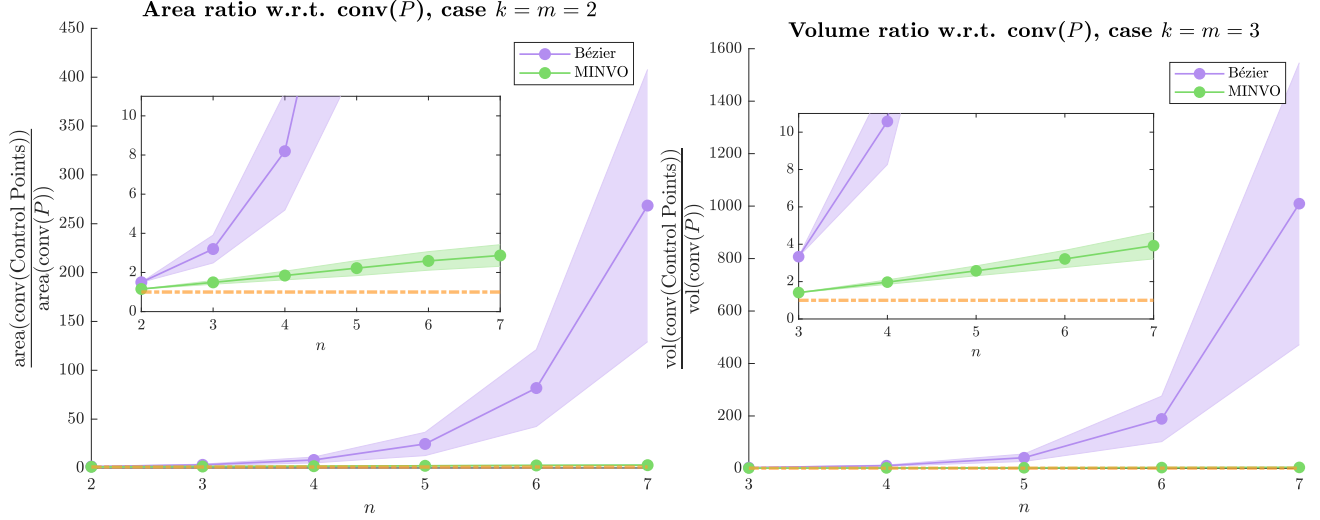


Fig. 12. Comparison of the convex hull of the MINVO and Bézier control points with respect to $\text{conv}(P)$ for the cases $k = m = 2$ (left) and $k = m = 3$ (right). For each n , a total of 10^3 polynomials passing through $n + 1$ random points in the cube $[-1, 1]^k$ were used. The shaded area is the 1σ interval, where σ is the standard deviation. The yellow dashed line marks a ratio of 1. Note how the growth of the ratio for the MINVO basis is approximately linear with n , while for the Bézier basis it is approximately exponential.

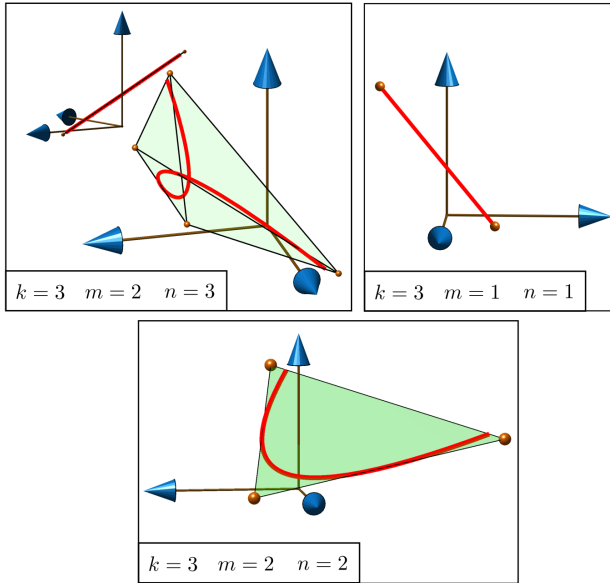


Fig. 13. The MINVO basis applied for different curves with $k = 3$ and different values of m and n : A cubic curve embedded in a two-dimensional subspace (top left), a segment embedded in a one-dimensional subspace (top right) and a quadratic curve embedded in a two-dimensional subspace (bottom).

that $V_{\text{MV}} < V_{\text{Be}}$ for any polynomial with $n > 3$, but the Monte Carlo results obtained show that this is true in most of the cases. For the case $n = 7$, the MINVO basis obtains convex hulls up to ≈ 550 times smaller than the Bézier basis.

Finally, we compare in Fig. 12 how these polyhedral convex hulls, obtained by either the MINVO or Bézier control points, approximate

$\text{conv}(P)$, which is the convex hull of the curve P . Similar to the previous cases, here we used a total of 10^3 polynomials passing through $n + 1$ points randomly sampled from the cube $[-1, 1]^k$. The error in the MINVO outer polyhedral approximation is approximately linear as n increases, but it is exponential for the Bézier basis. For instance, when $n = 7$ and $k = 3$, the Bézier control points generate a polyhedral outer approximation that is ≈ 1010 times bigger than the volume of $\text{conv}(P)$, while the a polyhedral outer approximation obtained by the MINVO control points is only ≈ 3.9 times bigger.

7.2 Rational Curves

Via projections, the MINVO basis is also able to obtain the smallest simplex that encloses some rational curves, which are curves whose coordinates are the quotients of two polynomials. For instance, given the simplex obtained by the MINVO basis for $n = 3$, we can project every point $p(t)$ of the curve via a perspective projection, using a vertex as the viewpoint, and the opposite face as the projection plane. Note that this perspective projection of the polynomial curve will be a rational curve. As MINVO obtains the smallest 3-simplex enclosing a polynomial curve, each face is guaranteed to be the smallest 2-simplex that encloses this 2D rational curve. This can be easily proven by contradiction, since if the face were not a minimal 2-simplex for the projected curve, then the 3-simplex would not be minimal for the original 3D curve (see [Sayrafiezadeh 1992] for instance).

Let us define the camera frame c as a frame that has z pointing from a vertex of the simplex to its opposite face, and the xy plane parallel to this face. Let f denote the distance between this vertex and its opposite face, and T_w^c denote the homogeneous transformation matrix (rotation and translation) that takes one point expressed in the world frame and transforms it to the camera frame. The projection is given in world coordinates $p_{\text{proj}}(t)$ by the standard

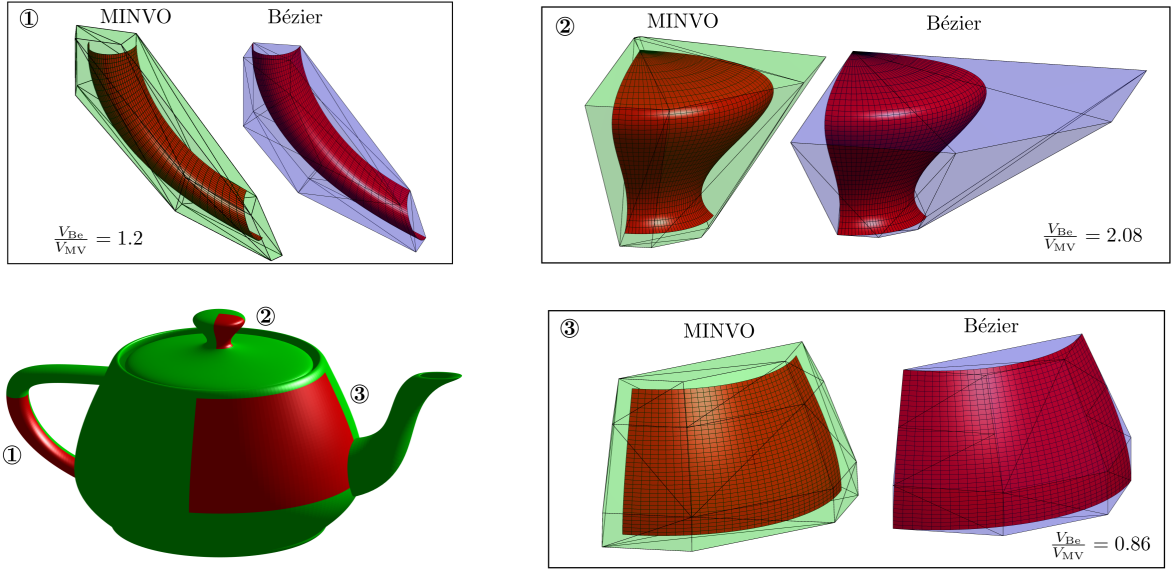


Fig. 14. Comparison of the MINVO and Bézier control points that generate three bicubic patches of the teapot on the left. The convex hull of the MINVO control points is larger for patch 3, but smaller for patches 1 and 2.

pinhole camera model [Carlone 2019]:

$$\begin{bmatrix} p_{\text{proj}}(t) & 1 \end{bmatrix}^T = (T_w^c)^{-1} \begin{bmatrix} q_1 & q_2 & f & 1 \end{bmatrix}^T$$

where

$$\begin{bmatrix} q_1 \\ q_2 \\ q_3 \end{bmatrix} := \begin{bmatrix} f & 0 & 0 \\ 0 & f & 0 \\ 0 & 0 & 1 \end{bmatrix} \begin{bmatrix} I_3 & 0 \end{bmatrix} T_w^c \begin{bmatrix} p(t) \\ 1 \end{bmatrix}$$

The four projections obtained for the case $n = 3$ are shown in Fig. 15. In this case, we use a 3D curve P that has $p(t) = [\lambda_1(t) \ \lambda_2(t) \ \lambda_3(t)]^T$, for which we know that the smallest enclosing simplex is the standard simplex $V = [0 \ I_3]$ (see also Fig. 2). P is projected onto the planes π_i using v_i as the viewpoint. Each face is then the smallest 2-simplex that encloses the projection, which is a rational curve.

7.3 Surfaces

Similar to any other polynomial basis that is nonnegative and is a partition of unity (i.e. the polynomials in the basis sum up to one), the MINVO basis can be applied to generate polynomial surfaces of degree (q, r) contained in \mathbb{R}^3 , which are defined by $(q+1) \cdot (r+1)$ control points. Let us define $u_q := [u^q \ u^{q-1} \ \dots \ 1]^T$ and let $A_{MV,q}$ denote the matrix A_{MV} for $n = q$. Analogous definitions apply for v , v_r , and $A_{MV,r}$. Moreover, let $V_{MV,j} \in \mathbb{R}^{(q+1) \times (r+1)}$ contain the coordinate $j \in \{x, y, z\}$ of the control points. The parametric equation of the surface will then be given by:

$$s(u, v) = \begin{bmatrix} (A_{MV,q} u_q)^T V_{MV,x} \\ (A_{MV,q} u_q)^T V_{MV,y} \\ (A_{MV,q} u_q)^T V_{MV,z} \end{bmatrix} A_{MV,r} v_r$$

where $s(u, v) \in \mathbb{R}^3$ and $u, v \in [-1, 1]$. An example of the MINVO

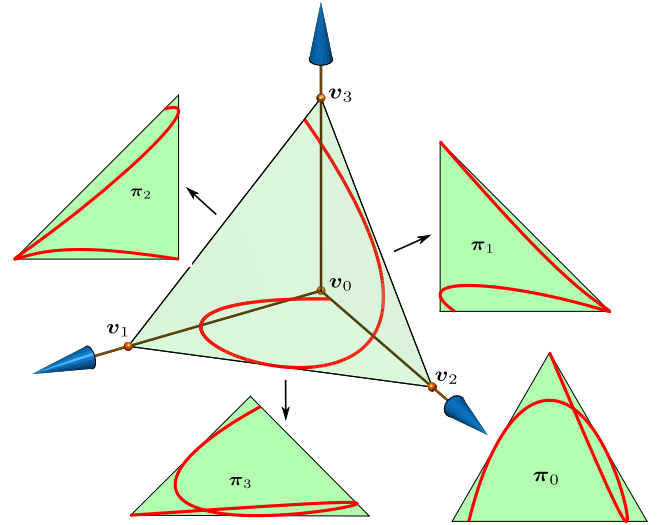


Fig. 15. The MINVO basis also obtains the smallest simplex that encloses some rational curves. In this case, the 3D curve is the curve obtained in Problem 2 for the standard simplex $V = [0 \ I_3]$. From the point of view of Problem 1, the standard simplex is the smallest 3-simplex containing the 3D curve in red. This means that each of its faces is also the smallest 2-simplex containing the projection of the curve onto each face π_i , using the opposite vertex v_i as viewpoint. These projections are rational curves (quotient of two polynomials).

basis applied to generate different bicubic surfaces (i.e., $q = r = 3$) is shown in Fig. 14. The control points used by the Bernstein/Bézier basis are also shown for comparison. In all these cases, the convex hull of the control points is guaranteed to enclose the surface. However, note that the MINVO basis is not guaranteed to produce the

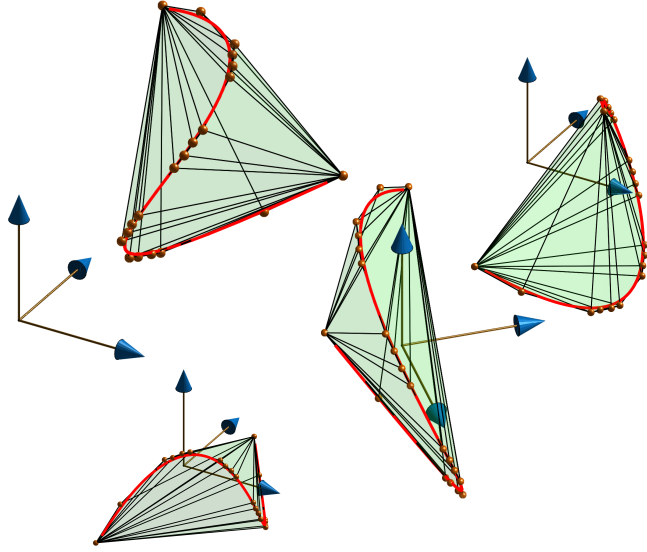


Fig. 16. Tighter polyhedral outer approximations for a curve $P \in \mathcal{P}^n$ can be obtained by splitting the curve into several intervals, calculating the MINVO n -simplices that enclose each one of these intervals and then computing the convex hull of all these simplices. In all these cases shown, the original curve $P \in \mathcal{P}^3$ is splitted into 5 intervals, and the resulting convex hull is a polyhedron with 20 vertexes that is 1.19 times smaller than the smallest 3-simplex that encloses the whole curve (i.e., the simplex found by applying the MINVO basis to the whole curve).

smallest polyhedron outer representation of the surface. A quantitative comparison of the volumes achieved by each one of the basis is shown in Fig. 14. Qualitatively, the MINVO basis is able to produce smaller polyhedral outer representations for “more curved” surfaces. Compare for example patch 2 and 3 in the figure: the convex hull of the MINVO control points for patch 3 (which is a more planar patch) is larger than the one of the Bézier control points. However, the convex hull of the MINVO control points of patch 2 is 2.08 times smaller than the one produced by the Bézier control points.

8 FINAL REMARKS

8.1 Tighter polyhedral volumes for Problem 1

Tighter polyhedral solutions for Problem 1 can be obtained by splitting the polynomial curve into several intervals and then computing the convex hull of the MINVO n -simplices that enclose each interval. Several examples for $n = 3$ are shown in Fig. 16, where the original curve $P \in \mathcal{P}^3$ is splitted into 5 intervals, and the resulting convex hull is a polyhedron with 20 vertexes that is 1.19 times smaller than the smallest 3-simplex that encloses the whole curve (i.e., the simplex found by applying the MINVO basis to the whole curve).

8.2 Conversion between MINVO, Bernstein and B-Spline

Given a curve $P \in \mathcal{P}^n$, the control points (i.e., the vertexes of the n -simplex that encloses that curve) using a basis α can be obtained from the control points of a different basis β ($\alpha, \beta \in \{\text{MV}, \text{Be}, \text{BS}\}$)

using the formula

$$V_\alpha = P(A_\alpha)^{-1} = V_\beta A_\beta (A_\alpha)^{-1}$$

For instance, to obtain the Bernstein control points from the MINVO control points we can use $V_{\text{Be}} = V_{\text{MV}} A_{\text{MV}} (A_{\text{Be}})^{-1}$. The matrices A_{MV} are the ones shown in Table 2, while the matrices A_{Be} and A_{BS} are available in [Qin 2000]. Note that all the matrices need to be expressed in the same interval ($t \in [-1, 1]$ in this paper). The code provided with this paper contains functions that generate all of these matrices.

Similarly, and using the definitions and notations of Section 7.3, the conversion between the control points of two basis α, β that define the same surface in \mathbb{R}^3 is given by:

$$V_{\beta,j} = \left(A_{\alpha,q} A_{\beta,q}^{-1} \right)^T V_{\alpha,j} A_{\alpha,r} A_{\beta,r}^{-1}$$

where $j \in \{x, y, z\}$.

9 CONCLUSIONS AND FUTURE WORK

This work derived and presented the MINVO basis. The key features of this basis is that it finds the smallest n -simplex that encloses a given n^{th} -order polynomial curve (Problem 1), and also finds the n^{th} -order polynomial curve with largest convex hull enclosed in a given n -simplex (Problem 2). For $n = 3$, the ratios of the improvement in the volume achieved by the MINVO basis with respect to the Bernstein and B-Spline bases are 2.36 and 254.9 respectively. When $n = 7$, these improvement ratios increase to 902.7 and $2.997 \cdot 10^{21}$ respectively. Global optimality was proven for $n = 1, 2, 3$. The MINVO basis was also applied to polynomial curves with different n, k and m (achieving improvements ratios of up to ≈ 550), polynomial surfaces and rational curves. All these results pave the way for much less conservative results (and hence much shorter computation times) in the algorithms of computer graphics, computer games, robotics and simulations that highly benefit from simplex approximations of a given polynomial curve.

The exciting results of this work naturally lead to the following questions and conjectures, that we leave as future work:

- Is the global optimum of Problem 4 the same as the global optimum of Problem 3? In other words, are we losing optimality by imposing the specific structure in $\lambda_i(t)$? The results seem to indicate that it is likely that no optimality is lost.
- Does there exist a recursive formula to obtain the solution of Problem 3 for a specific $n = q$ given the previous solutions for $n = 1, \dots, q - 1$? Would this recursive formula allow to obtain the *globally* optimal solutions $\forall n$ of Problem 3?

ACKNOWLEDGMENTS

The authors would like to thank Prof. Gilbert Strang, Prof. Johan Löfberg, Ashkan M. Jasour, Kasra Khosoussi, Kaveh Fathian, Michael Everett, Juan José Madrigal and Marc Adillón for helpful insights and discussions. Thanks also to Parker Lusk, Kris Frey, Stewart Jamieson, Joe Basconi, and Maodong Pan for their great comments on this paper. Research funded in part by Boeing Research & Technology.

REFERENCES

- Autocad®. 2020. Autodesk® Autocad®. <https://www.autodesk.com/products/autocad/>
- Adam W Bargteil and Elaine Cohen. 2014. Animation of deformable bodies with quadratic Bézier finite elements. *ACM Transactions on Graphics (TOG)* 33, 3 (2014), 1–10.
- Constantin Carathéodory. 1907. Über den Variabilitätsbereich der Koeffizienten von Potenzreihen, die gegebene Werte nicht annehmen. *Math. Ann.* 64, 1 (1907), 95–115.
- Luca Carlone. 2019. Lecture notes on Image Formation, Visual Navigation for Autonomous Vehicles.
- Venanzio Cichella, Isaac Kaminer, Claire Walton, and Naira Hovakimyan. 2017. Optimal motion planning for differentially flat systems using Bernstein approximation. *IEEE Control Systems Letters* 2, 1 (2017), 181–186.
- Daniel Ciripoi, Nidhi Kaihnsa, Andreas Löhne, and Bernd Sturmfels. 2018. Computing convex hulls of trajectories. *arXiv preprint arXiv:1810.03547* (2018).
- Thao Dang and Romain Testylier. 2012. Reachability Analysis for Polynomial Dynamical Systems Using the Bernstein Expansion. *Reliab. Comput.* 17, 2 (2012), 128–152.
- Eric A De Kemp. 1999. Visualization of complex geological structures using 3-D Bezier construction tools. *Computers & Geosciences* 25, 5 (1999), 581–597.
- Douglas Derry. 1956. Convex hulls of simple space curves. *Canadian Journal of Mathematics* 8 (1956), 383–388.
- E Dimas and D Briassoulis. 1999. 3D geometric modelling based on NURBS: a review. *Advances in Engineering Software* 30, 9–11 (1999), 741–751.
- Alexander Efremov, Vlastimil Havran, and Hans-Peter Seidel. 2005. Robust and numerically stable Bézier clipping method for ray tracing NURBS surfaces. In *Proceedings of the 21st spring conference on Computer graphics*. 127–135.
- Christer Ericson. 2004. *Real-time collision detection*. CRC Press.
- Michael Everett, Bjorn Lutjens, and Jonathan P How. 2020. Certified Adversarial Robustness for Deep Reinforcement Learning. *arXiv preprint arXiv:2004.06496* (2020).
- Julian J Faraway, Matthew P Reed, and Jing Wang. 2007. Modelling three-dimensional trajectories by using Bézier curves with application to hand motion. *Journal of the Royal Statistical Society: Series C (Applied Statistics)* 56, 5 (2007), 571–585.
- Daniel Galicer, Mariano Merzbacher, and Damián Pinasco. 2019. The minimal volume of simplices containing a convex body. *The Journal of Geometric Analysis* 29, 1 (2019), 717–732.
- Jürgen Garloff and Andrew P Smith. 2003. A comparison of methods for the computation of affine lower bound functions for polynomials. In *International Workshop on Global Optimization and Constraint Satisfaction*. Springer, 71–85.
- Elmer G Gilbert, Daniel W Johnson, and S Sathiya Keerthi. 1988. A fast procedure for computing the distance between complex objects in three-dimensional space. *IEEE Journal on Robotics and Automation* 4, 2 (1988), 193–203.
- Philip E. Gill, Walter Murray, and Michael A. Saunders. 2005. SNOPT: An SQP algorithm for large-scale constrained optimization. *SIAM Rev.* 47 (2005), 99–131.
- Philip E. Gill, Walter Murray, Michael A. Saunders, and Elizabeth Wong. 2018. *User's Guide for SNOPT 7.7: Software for Large-Scale Nonlinear Programming*. Center for Computational Mathematics Report CCoM 18-1. Department of Mathematics, University of California, San Diego, La Jolla, CA.
- Eligius MT Hendrix, Inmaculada García, Javier Plaza, and Antonio Plaza. 2013. On the minimum volume simplex enclosure problem for estimating a linear mixing model. *Journal of Global Optimization* 56, 3 (2013), 957–970.
- Gary Herron. 1989. Polynomial bases for quadratic and cubic polynomials which yield control points with small convex hulls. *Computer aided geometric design* 6, 1 (1989), 1–9.
- Inventor®. 2020. Autodesk® Inventor®. <https://www.autodesk.com/products/inventor/>
- Marian-Daniel Iordache, José Bioucas-Dias, and António Plaza. 2009. Unmixing sparse hyperspectral mixtures. In *2009 IEEE International Geoscience and Remote Sensing Symposium*, Vol. 4. IEEE, IV–85.
- KG Jolly, R Sreerama Kumar, and R Vijayakumar. 2009. A Bezier curve based path planning in a multi-agent robot soccer system without violating the acceleration limits. *Robotics and Autonomous Systems* 57, 1 (2009), 23–33.
- Atsushi Kanazawa. 2014. On the minimal volume of simplices enclosing a convex body. *Archiv der Mathematik* 102, 5 (2014), 489–492.
- Samuel Karlin and Lloyd S Shapley. 1953. *Geometry of moment spaces*. Number 12. American Mathematical Soc.
- Victor Klee. 1986. Facet-centroids and volume minimization. *Studia Scientiarum Mathematicarum Hungarica* 21 (1986), 143–147.
- Mark Grigorevich Krein, D Louvish, et al. 1977. *The Markov moment problem and extremal problems*. American Mathematical Society.
- József Kuti, Péter Galambos, and Péter Baranyi. 2014. Minimal Volume Simplex (MVS) approach for convex hull generation in TP Model Transformation. In *IEEE 18th International Conference on Intelligent Engineering Systems INES 2014*. IEEE, 187–192.
- J. B. Lasserre. 2001. Global optimization with polynomials and the problem of moments. *SIAM Journal on Optimization* 11, 3 (2001), 796–817.
- Johan Löfberg. 2020. Envelope approximations for global optimization. <https://yalmip.github.io/tutorial/envelopesinmbmbnb/>.
- Jun Li and José M Bioucas-Dias. 2008. Minimum volume simplex analysis: A fast algorithm to unmix hyperspectral data. In *IGARSS 2008-2008 IEEE International Geoscience and Remote Sensing Symposium*, Vol. 3. IEEE, III–250.
- J. Löfberg. 2004. YALMIP : A Toolbox for Modeling and Optimization in MATLAB. In *In Proceedings of the CACSD Conference*. Taipei, Taiwan.
- Johan Löfberg. 2009. Pre- and post-processing sum-of-squares programs in practice. *IEEE Trans. Automat. Control* 54, 5 (2009), 1007–1011.
- MATLAB Optimization Toolbox 2020. MATLAB Optimization Toolbox. The MathWorks, Natick, MA, USA.
- Maya®. 2020. Autodesk® Maya®. <https://www.autodesk.com/products/maya/>
- Kostyantyn Mazur. 2017. Convex Hull of (t, t^2, \dots, t^N) . *arXiv preprint arXiv:1706.02060* (2017).
- FC Park and Bahram Ravani. 1995. Bézier curves on Riemannian manifolds and Lie groups with kinematics applications. (1995).
- Pablo Parrilo. 2006. Lecture notes in Algebraic Techniques and Semidefinite Optimization.
- James A Preiss, Karol Hausman, Gaurav S Sukhatme, and Stephan Weiss. 2017. Trajectory Optimization for Self-Calibration and Navigation.. In *Robotics: Science and Systems*.
- Kaihuai Qin. 2000. General matrix representations for B-splines. *The Visual Computer* 16, 3–4 (2000), 177–186.
- Kristian Ranestad and Bernd Sturmfels. 2009. On the convex hull of a space curve. *arXiv preprint arXiv:0912.2986* (2009).
- Derek M Rogge, Benoit Rivard, Jinkai Zhang, and Jilu Feng. 2006. Iterative spectral unmixing for optimizing per-pixel endmember sets. *IEEE Transactions on Geoscience and Remote Sensing* 44, 12 (2006), 3725–3736.
- Tae Roh and Lieven Vandenbergh. 2006. Discrete transforms, semidefinite programming, and sum-of-squares representations of nonnegative polynomials. *SIAM Journal on Optimization* 16, 4 (2006), 939–964.
- SH Roth, Markus H Gross, Silvio Turello, and Friedrich R Carls. 1998. A Bernstein-Bézier Based Approach to Soft Tissue Simulation. In *Computer Graphics Forum*, Vol. 17. Wiley Online Library, 285–294.
- Ozgur Koray Sahingoz. 2014. Generation of Bézier curve-based flyable trajectories for multi-UAV systems with parallel genetic algorithm. *Journal of Intelligent & Robotic Systems* 74, 1–2 (2014), 499–511.
- M Sayrafiezadeh. 1992. An Inductive Proof for Extremal Simplexes. *Mathematics Magazine* 65, 4 (1992), 252–255.
- Christian Schulz. 2009. Bézier clipping is quadratically convergent. *Computer Aided Geometric Design* 26, 1 (2009), 61–74.
- Thomas W Sederberg and Tomoyuki Nishita. 1990. Curve intersection using Bézier clipping. *Computer-Aided Design* 22, 9 (1990), 538–549.
- Vyacheslav D Sedykh. 1986. Structure of the convex hull of a space curve. *Journal of Soviet Mathematics* 33, 4 (1986), 1140–1153.
- Igor Škrjanc and Gregor Klančar. 2010. Optimal cooperative collision avoidance between multiple robots based on Bernstein-Bézier curves. *Robotics and Autonomous systems* 58, 1 (2010), 1–9.
- Ernst Steinitz. 1913. Bedingt konvergente Reihen und konvexe Systeme. *Journal für die reine und angewandte Mathematik (Crelles Journal)* 1913, 143 (1913), 128–176.
- Gabor Szeg. 1939. *Orthogonal polynomials*. Vol. 23. American Mathematical Soc.
- Jesus Tordesillas, Brett T Lopez, and Jonathan P How. 2019. FASTER: Fast and Safe Trajectory Planner for Flights in Unknown Environments. In *2019 IEEE/RSJ International Conference on Intelligent Robots and Systems (IROS)*. IEEE.
- Tatsumi Uezato, Mathieu Fauvel, and Nicolas Dobigeon. 2019. Hyperspectral unmixing with spectral variability using adaptive bundles and double sparsity. *IEEE Transactions on Geoscience and Remote Sensing* 57, 6 (2019), 3980–3992.
- Gert Vegter and Chee Yap. 1993. Finding minimal circumscribing simplices Part 1: Classifying local minima. (1993).
- Miguel Velez-Reyes, Angela Puetz, Michael P Hoke, Ronald B Lockwood, and Samuel Rosario. 2003. Iterative algorithms for unmixing of hyperspectral imagery. In *Algorithms and Technologies for Multispectral, Hyperspectral, and Ultraspectral Imagery IX*, Vol. 5093. International Society for Optics and Photonics, 418–429.
- Eric Wong and Zico Kolter. 2018. Provable defenses against adversarial examples via the convex outer adversarial polytope. In *International Conference on Machine Learning*. 5286–5295.
- Yunhong Zhou and Subhash Suri. 2002. Algorithms for a minimum volume enclosing simplex in three dimensions. *SIAM J. Comput.* 31, 5 (2002), 1339–1357.

A VOLUME OF THE CONVEX HULL OF A POLYNOMIAL CURVE

The volume for any n -th order polynomial curve can be easily obtained using the result from [Karlin and Shapley 1953, Theorem 15.2]. In this work⁴, it is shown that the volume of the convex hull of a curve R with $\mathbf{r}(t) := \left[\frac{t+1}{2} \left(\frac{t+1}{2} \right)^2 \cdots \left(\frac{t+1}{2} \right)^n \right]^T$ is given by

$$\text{vol}(\text{conv}(R)) = \prod_{j=1}^n B(j, j) = \prod_{j=1}^n \left(\frac{((j-1)!)^2}{(2j-1)!} \right) = \frac{1}{n!} \prod_{j=1}^n \left(\frac{j!(j-1)!}{(2j-1)!} \right) = \frac{1}{n!} \prod_{0 \leq i < j \leq n} \left(\frac{j-i}{j+i} \right)$$

where $B(x, y)$ denotes the beta function. Let us now define $\tilde{\mathbf{t}}$ as $\tilde{\mathbf{t}} := [t^n \ t^{n-1} \ \cdots \ t]^T$, \boxtimes as any number $\in \mathbb{R}$ and write $\mathbf{r}(t)$ as:

$$\mathbf{r}(t) = \underbrace{\begin{bmatrix} 0 & 0 & \cdots & 0 & \frac{1}{2} & \boxtimes \\ 0 & 0 & \cdots & \frac{1}{2^2} & \boxtimes & \boxtimes \\ \vdots & \vdots & \ddots & \vdots & \vdots & \vdots \\ 0 & \frac{1}{2^{n-1}} & \cdots & \boxtimes & \boxtimes & \boxtimes \\ \frac{1}{2^n} & \boxtimes & \cdots & \boxtimes & \boxtimes & \boxtimes \end{bmatrix}}_{:=R} \mathbf{t} = R_{:,0:n-1} \tilde{\mathbf{t}} + R_{:,n}$$

Now, defining $Q := P_{:,0:n-1} R_{:,0:n-1}^{-1}$, note that $(\mathbf{p}(t) - P_{:,n}) = P_{:,0:n-1} \tilde{\mathbf{t}} = Q R_{:,0:n-1} \tilde{\mathbf{t}} = Q(\mathbf{r}(t) - R_{:,n}) = Q\mathbf{r}(t) - Q R_{:,n}$. As the translation part does not affect the volume, we can write:

$$\text{vol}(\text{conv}(P)) = \text{vol}(\text{conv}(\{\mathbf{p}(t) - P_{:,n} \mid t \in [-1, 1]\})) = \text{vol}(\text{conv}(\{Q\mathbf{r}(t) \mid t \in [-1, 1]\})) = \dots$$

$$\dots = \text{vol}(Q\text{conv}(R)) = \text{abs} \left(\frac{|P_{:,0:n-1}|}{|R_{:,0:n-1}|} \right) \text{vol}(\text{conv}(R))$$

where we have used the notation $Q\text{conv}(R)$ to denote the set $\{Q\mathbf{x} \mid \mathbf{x} \in \text{conv}(R)\}$.

As the determinant of $R_{:,0:n-1}$ is $|R_{:,0:n-1}| = \prod_{i=1}^n \frac{1}{2^i} = 2^{-\frac{n(n+1)}{2}}$, we can conclude that:

$$\text{vol}(\text{conv}(P)) = \frac{\text{abs}(|P_{:,0:n-1}|)}{n!} 2^{\frac{n(n+1)}{2}} \prod_{0 \leq i < j \leq n} \left(\frac{j-i}{j+i} \right)$$

□

B INVERTIBILITY OF THE MATRIX A

From Eq. 3, we have that the $(n+1) \times (n+1)$ matrix A satisfies

$$\begin{bmatrix} P \\ \mathbf{e}^T \end{bmatrix} = \begin{bmatrix} V \\ \mathbf{1}^T \end{bmatrix} A$$

As $\text{abs} \left(\begin{bmatrix} P \\ \mathbf{e}^T \end{bmatrix} \right) = \text{abs}(|P_{:,0:n-1}|) \neq 0$, and $\left| \begin{bmatrix} V \\ \mathbf{1}^T \end{bmatrix} \right| = |V^T \mathbf{1}| \neq 0$ (see Section 4), we have that $\text{rank} \left(\begin{bmatrix} P \\ \mathbf{e}^T \end{bmatrix} \right) = \text{rank} \left(\begin{bmatrix} V \\ \mathbf{1}^T \end{bmatrix} \right) = n+1$. Using now the fact that $\text{rank}(BC) \leq \min(\text{rank}(B), \text{rank}(C))$, we conclude that $\text{rank}(A) = n+1$ (i.e. A has full rank), and therefore A is invertible. □

C KARUSH-KUHN-TUCKER CONDITIONS (FOR ODD n)

In this Appendix we derive the KKT conditions for this problem:

$$\begin{array}{ll} \min_{A \in \mathbb{R}^{(n+1) \times (n+1)}} & -\ln(|A^T A|) \\ \text{s.t.} & A^T \mathbf{1} = \mathbf{e} \\ & A\mathbf{t} \geq \mathbf{0} \quad \forall t \in [-1, 1] \end{array}$$

which is equivalent to Problem 3. For the sake of brevity, we present here the case n odd (the case n even can be easily obtained with small modifications). In the following, $V * W$ will be the matrix resulting from the row-wise discrete convolution (i.e. $(V * W)_{i,:} = V_{i,:} * W_{i,:}$), and

⁴Note that [Karlin and Shapley 1953] uses the convention $t \in [0, 1]$ (instead of $t \in [-1, 1]$), and therefore it uses the curve $[t \ t^2 \ \cdots \ t^n]^T$

$\text{Top}(\mathbf{a}, \mathbf{b})$ will denote the Toeplitz matrix whose first column is \mathbf{a} and whose first row is \mathbf{b}^T . Let us also define:

$$\mathbf{R}_G := \text{Top}\left(\begin{bmatrix} 1 \\ 1 \\ \mathbf{0}_{n-1} \end{bmatrix}, \begin{bmatrix} 1 \\ \mathbf{0}_{n-1} \end{bmatrix}\right) = \begin{bmatrix} \mathbf{I}_n \\ \mathbf{0}_n^T \end{bmatrix} + \begin{bmatrix} \mathbf{0}_n^T \\ \mathbf{I}_n \end{bmatrix} \quad \mathbf{R}_H := \text{Top}\left(\begin{bmatrix} -1 \\ 1 \\ \mathbf{0}_{n-1} \end{bmatrix}, \begin{bmatrix} -1 \\ \mathbf{0}_{n-1} \end{bmatrix}\right) = \begin{bmatrix} -\mathbf{I}_n \\ \mathbf{0}_n^T \end{bmatrix} + \begin{bmatrix} \mathbf{0}_n^T \\ \mathbf{I}_n \end{bmatrix} \quad \mathbf{L}_q := \begin{bmatrix} \mathbf{0}^T & \mathbf{0} \\ \mathbf{I}_{q-1} & \mathbf{0} \end{bmatrix}_{q \times q}$$

and the matrices $\mathbf{G} \in \mathbb{R}^{(n+1) \times \frac{n+1}{2}}$, $\mathbf{H} \in \mathbb{R}^{(n+1) \times \frac{n+1}{2}}$ and $\boldsymbol{\lambda} \in \mathbb{R}^{(n+1)}$. We know that:

$$\begin{aligned} (\mathbf{A}t)_i \geq 0 \quad \forall t \in [-1, 1] &\iff (\mathbf{A}t)_i = (t+1)g_i^2(t) + (1-t)h_i^2(t) \iff (\mathbf{A}t)_i = (\mathbf{G}_{i,:} * \mathbf{G}_{i,:}) \mathbf{R}_G^T + (\mathbf{H}_{i,:} * \mathbf{H}_{i,:}) \mathbf{R}_H^T \iff \\ &\dots \iff \mathbf{A} = \begin{bmatrix} \mathbf{G} * \mathbf{G} & \mathbf{H} * \mathbf{H} \end{bmatrix} \begin{bmatrix} \mathbf{R}_G^T \\ \mathbf{R}_H^T \end{bmatrix} \end{aligned} \quad (4)$$

where $g_i(t)$ and $h_i(t)$ are polynomials of degree $\frac{n-1}{2}$. Note that (a) is given by the Markov–Lukács theorem (see Section 5.4). In (b) we have simply used the discrete convolution to multiply $g_i(t)$ by itself, and the Toeplitz matrix \mathbf{R}_G to multiply the result by $(t+1)$ [Qin 2000]. An analogous reasoning applies for the term with h_i^5 . Using now \mathbf{G} and \mathbf{H} as the decision variables of the primal problem (where \mathbf{A} is given by Eq. 4), the Lagrangian is:

$$\mathcal{L} = -\ln(|\mathbf{A}^T \mathbf{A}|) + \boldsymbol{\lambda}^T (\mathbf{A}^T \mathbf{1} - \mathbf{e})$$

Differentiating the Lagrangian yields to:

$$\frac{\partial \mathcal{L}}{\partial G_{ij}} = \text{tr} \left(- \underbrace{\frac{\partial \ln(|\mathbf{A}^T \mathbf{A}|)}{\partial \mathbf{A}}}_{=2\mathbf{A}^* = 2\mathbf{A}^{-1}} \mathbf{Q}_{G_{ij}} \right) + \text{tr}(\boldsymbol{\lambda} \mathbf{1}^T \mathbf{Q}_{G_{ij}}) = \text{tr} \left((-2\mathbf{A}^{-1} + \boldsymbol{\lambda} \mathbf{1}^T) \mathbf{Q}_{G_{ij}} \right)$$

where

$$\mathbf{Q}_{G_{ij}} := \frac{\partial \mathbf{A}}{\partial G_{ij}} = 2 \left(\mathbf{L}_{(n+1)} \right)^{i-1} \begin{bmatrix} \mathbf{G}_{i,:} & \mathbf{0}^T \\ \mathbf{0}_{n \times (n+1)} \end{bmatrix} \begin{bmatrix} \mathbf{L}_n^T \\ \mathbf{0}_{(n+1) \times (n+1)} \end{bmatrix}^j \mathbf{R}_G^T \quad (5)$$

Same expression applies for $\mathbf{Q}_{H_{ij}} := \frac{\partial \mathbf{A}}{\partial H_{ij}}$, but using $\mathbf{H}_{i,:}$ and \mathbf{R}_H^T instead. The KKT equations can therefore be written as follows:

KKT equations: Solve for $\mathbf{G}, \mathbf{H}, \boldsymbol{\lambda}$:

$$\begin{cases} \text{tr} \left((-2\mathbf{A}^{-1} + \boldsymbol{\lambda} \mathbf{1}^T) \mathbf{Q}_{G_{ij}} \right) = 0 & \forall i \in \{0, \dots, n\}, \forall j \in \{0, \dots, \frac{n-1}{2}\} \\ \text{tr} \left((-2\mathbf{A}^{-1} + \boldsymbol{\lambda} \mathbf{1}^T) \mathbf{Q}_{H_{ij}} \right) = 0 & \forall i \in \{0, \dots, n\}, \forall j \in \{0, \dots, \frac{n-1}{2}\} \\ \mathbf{A}^T \mathbf{1} = \mathbf{e} \end{cases}$$

where \mathbf{A} is given by Eq. 4. and $\mathbf{Q}_{G_{ij}}$ by Eq. 5. $\mathbf{Q}_{H_{ij}}$ is also given by Eq. 5, but using $\mathbf{H}_{i,:}$ and \mathbf{R}_H^T instead.

⁵Alternatively, we can also write:

$$(\mathbf{A}_{i,:})^T = \mathbf{R}_G \text{Top} \left(\begin{bmatrix} \mathbf{G}_{i,:} \\ \mathbf{0}_{\frac{n-1}{2}} \end{bmatrix}, \begin{bmatrix} \mathbf{G}_{i,0} \\ \mathbf{0}_{\frac{n-1}{2}} \end{bmatrix} \right) \mathbf{G}_{i,:} + \mathbf{R}_H \text{Top} \left(\begin{bmatrix} \mathbf{H}_{i,:} \\ \mathbf{0}_{\frac{n-1}{2}} \end{bmatrix}, \begin{bmatrix} \mathbf{H}_{i,0} \\ \mathbf{0}_{\frac{n-1}{2}} \end{bmatrix} \right) \mathbf{H}_{i,:}$$